https://doi.org/10.1070/RCR4900

Lower olefins from methane: recent advances

Natalya V. Kolesnichenko, Natalya N. Ezhova, Yulya M. Snatenkova

A.V.Topchiev Institute of Petrochemical Synthesis of the Russian Academy of Sciences, Leninsky prosp. 29, 119991 Moscow, Russian Federation

Modern methods for methane conversion to lower olefins having from 2 to 4 carbon atoms per molecule are generalized. Multistage processing of methane into ethylene and propylene *via* syngas or methyl chloride and methods for direct conversion of CH_4 to ethylene are described. Direct conversion of syngas to olefins as well as indirect routes of the process *via* methanol or dimethyl ether are considered. Particular attention is paid to innovative methods of olefin synthesis. Recent achievements in the design of catalysts and development of new techniques for efficient implementation of oxidative coupling of methane and methanol conversion to olefins are analyzed and systematized. Advances in commercializing these processes are pointed out. Novel catalysts for Fischer – Tropsch synthesis of lower olefins from syngas and for innovative technique using oxide – zeolite hybrid catalytic systems are described. The promise of a new route to lower olefins by methane conversion *via* dimethyl ether is shown. Prospects for the synthesis of lower olefins *via* methyl chloride and using non-oxidative coupling of methane are discussed. The most efficient processes used for processing of methane to lower olefins are compared on the basis of degree of conversion of carbonaceous feed, possibility to integrate with available full-scale production, number of reaction stages and thermal load distribution.
The bibliography includes 346 references.

Contents

1. Introduction 191
2. Lower olefins from methane *via* syngas and methanol 193
3. Lower olefins from methane *via* syngas and dimethyl ether 196
4. Catalysts for the synthesis of lower olefins from methanol and dimethyl ether 198
   4.1. Catalysts based on SAPO-34 198
   4.2. Catalysts based on ZSM-5 zeolites 200
   4.3. Catalysts based on nanosized ZSM-5 zeolites 200
   4.4. Post-synthetic treatment of ZSM-5 to prepare nanosized zeolites 204
5. Lower olefins from methane *via* syngas using the Fischer – Tropsch and OX – ZEO methods 205
6. Ethylene and propylene from methane *via* methyl halides 208
7. Oxidative coupling of methane to ethylene 211
8. Non-oxidative coupling of methane to ethylene 215
9. Conclusion 216

1. Introduction

Lower olefins including ethylene, propylene and butenes are key intermediates of full-scale petrochemical and organic synthesis. They serve a basis for production of a broad spectrum of chemical products from plastics to anti-freezing liquids and solvents.[1] Ethylene is mainly consumed in the large-scale synthesis of polyethylene, polyvinyl chloride, ethylene oxide, ethanol, acetaldehyde, glycols, vinyl acetate, ethylbenzene and styrene. Propylene is used to obtain polypropylene, modified polymers, propylene oxide, acrylonitrile and acrylic acid, cumene, isopropyl alcohol and oxo alcohols. Butenes are used as reactants for the synthesis of butyl alcohol, maleic anhydride, polybutylene and as co-monomers in the synthesis of low-density polyethylene.

The development of the olefin sector of industry is driven by global economic growth and increased demand for consumer goods (especially, polymeric materials).[2] By 2016, the world production of lower olefins $C_2^= - C_4^=$ reached 260 mln tonnes annually.[2] Among them, ethylene and propylene are especially in demand on the chemical market; they account for over 96% of the overall production of olefins. The demand for ethylene and propylene continuously increases,[3–6] *viz.*, the production volume of these chemicals doubled since 2000 (Fig. 1).

For more than nine decades lower olefins were obtained by pyrolysis of naphtha (product of petroleum distillation). However, to date the conventional technology reached its limit and cannot fulfill increasing demands of the petrochemical industry for olefins.[2] The available petroleum resources significantly decreased, while petroleum prices are volatile.[1,7]

There has been a trend towards diversification of the hydrocarbon resource base in the olefin complex since the beginning of the 21st century.[8] Namely, oil is gradually replaced by natural gas, the cheapest large-scale hydrocarbon resource whose estimated reserves are huge (>550 trillion m^3).[9] Transition from oil to gas allows the olefin

Received 20 May 2019

© 2020 Uspekhi Khimii, ZIOC RAS, Russian Academy of Sciences and IOP Publishing Limited

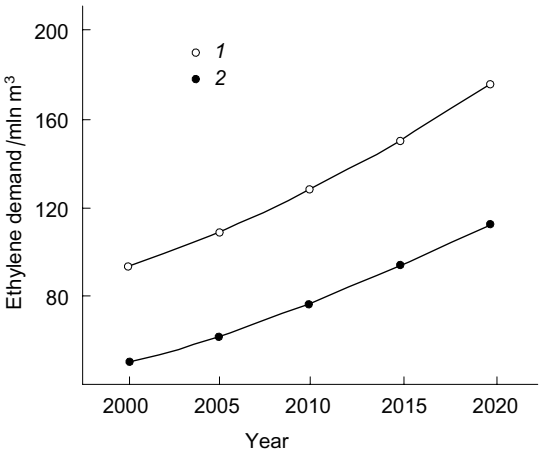


Figure 1. Changes in ethylene (*1*) and propylene (*2*) demand on global olefin market in the last two decades.[2,4–6]

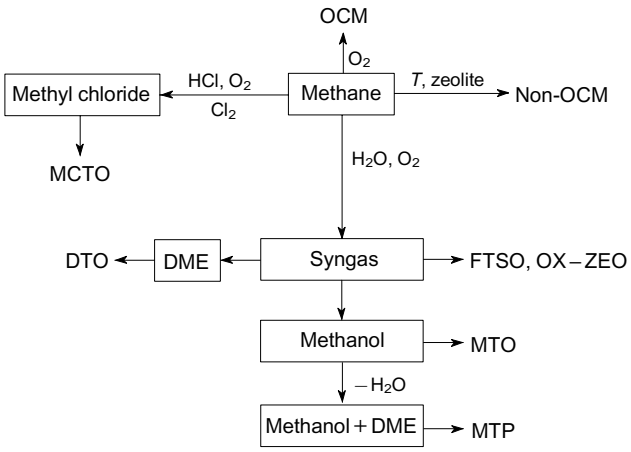


Figure 2. Methods for methane conversion to lower olefins. Method: OCM is oxidative coupling of methane, Non-OCM is non-oxidative coupling of methane, MCTO is methyl chloride to olefins, DTO is dimethyl ether (DME) to olefins, FTSO is Fischer–Tropsch synthesis of olefins, OX–ZEO is oxide–zeolite method, MTO is methanol to olefins, and MTP is methanol to propylene.

plants to significantly reduce raw material costs (by at least 3.5 times).[10] In turn, processing of natural gas to olefins is also of interest for natural gas chemical industry. This is a very effective way to monetize natural gas. Indeed, conversion of natural gas to ethylene and propylene causes the cost of production to increase by 7 to 9 times and even by 17 to 20 times provided subsequent production of polymers.[10] Construction of natural gas processing plants is particularly topical in countries with continuously growing overproduction of natural gas (USA, Russian Federation).

To date, nearly 30% of olefin plants in the world use natural gas as hydrocarbon raw material. In the USA, the proportion of natural gas in the olefin sector of industry is more than 40%, and it is planned to minimize the use of crude oil in the future.[8]

However, natural gas chemical industry mainly uses the ethane–propane component of natural gas. As a consequence, only 3%–15% of hydrocarbon raw material is converted to petrochemicals while the major, methane, component (55%–99%) is unaffected. Since natural gas processing technologies utilize only combination gas (shale gas, associated petroleum gas, *etc.*), more than 350 trillion m^3 of the methane component of natural gas remain untouched.[9]

Abundance of methane on the global market pushes the interest in the development of processes for methane conversion to valuable chemical products.[8,11–14] Numerous methods were proposed to obtain lower olefins from the major component of natural gas, including both one-stage and multistage processes (Fig. 2) and different techniques of the primary activation of CH_4 molecule:

— activation by oxygen on oxide catalysts — oxidative coupling of methane to ethylene and ethane (OCM);

— activation by thermocatalytic decomposition of CH_4 molecule on the surface of zeolite or oxide catalysts (non-oxidative coupling of methane to hydrocarbons, or Non-OCM);

— activation *via* methane reforming to syngas followed by syngas conversion to olefins by the Fischer–Tropsch (FTSO) and oxide–zeolite (OX–ZEO) methods, *via* methanol (MTO) or dimethyl ether (DTO), or *via* a methanol–dimethyl ether mixture (MTP); and

— activation *via* chlorination or oxidative chlorination followed by methyl chloride conversion to olefins (MCTO).

Recently, all these processes for methane conversion to lower olefins have been intensively developed by large companies including Honeywell, Lurgi, INEOS (Inspec Ethylene Oxide Specialities), Total, JGC Corp. (Japan Gasoline Corp,), Mitsubishi, Sabic Global Technology, *etc.*, as well as at certain research centres in Russia and abroad. A few dozens of articles and patents that describe new experimental data and theoretical results appear yearly.

The results reported before 2016 were generalized in part in a review[8] that was mainly devoted to certain methods for the synthesis of olefins. Most reviews are concerned with OCM.[12,15–18] These works include a considerable body of information on catalysts,[15,18] innovative technologies[11,16] and the OCM kinetics and mechanism.[12,15] The results of intensive studies on methanol conversion to olefins were analyzed in the review articles[19–25] concerned with new catalysts,[19–20] specific features of the reaction mechanism,[21–24] various aspects of scaling up process[25] and commercialization[20,25] of the MTO and MTP processes. Advances in the development of processes of olefin production using the Fischer–Tropsch method[8] or *via* DME[24,26,27] have been poorly documented so far (usually, the results obtained are compared with those obtained using the MTO approach). New interesting results of studies on methane conversion to olefins *via* methyl chloride[28,29] or

N.V.Kolesnichenko. Doctor of Chemical Sciences, Professor, Chief Researcher of the TIPS RAS.
Telephone: +7(495)647–5927 (ext. 1-97), e-mail: nvk@ips.ac.ru
N.N.Ezhova. PhD (Chemistry), Leading Researcher of the TIPS RAS.
Telephone: +7(495)647–5927 (ext. 1-97), e-mail: nnejova@mail.ru
Yu.M.Snatenkova. Junior Researcher of the TIPS RAS.
Telephone: +7(495)647–5927 (ext. 1-97), e-mail: snatenkova@ips.ac.ru
Current research interests of the authors: natural gas chemistry, methane processing into hydrocarbons (ethylene, propylene, gasoline, aromatic hydrocarbons), catalytic synthesis of lower olefins from dimethyl ether, heterogeneous catalysis, catalysts based on zeolites, nanosized catalysts, nanotechnology.

Translation: A.M.Raevskiy

using the Non-OCM reaction[11,12,30,31] remain almost unsystematized.

The aim of this review is to outline recent advances in the development of methods for processing of methane to lower olefins ($C_2^=-C_4^=$), to formulate general trends of progress in the title field and to characterize high-performance catalysts and processes that are of interest for potential industrial applications in the future.

To date, various methods for conversion of methane to lower olefins have been proposed (see Fig. 2). However, only the processes proceeding *via* syngas and methanol (MTO and MTP processes, respectively) have been best developed and industrialized. All other methods are either under laboratory testing or in the first pilot testing phase.

Notations are as follows:

$C_2^=$ — ethylene;

$C_2^=-C_4^=$ — lower olefins having from two to four carbon atoms per molecule;

$C_3^=$ — propylene;

$C_4^=$ — butenes;

C_{4+} — hydrocarbons having at least four carbon atoms per molecule;

DICP — Dalian Institute of Chemical Physics (China);

DME — dimethyl ether;

DMTO — DICP methanol to olefins method;

DTO — dimethyl ether to olefins method;

DTP — dominant technology for the propylene production;

INEOS — inspec ethylene oxide specialities;

FMTP — fluidized methanol to propylene;

FTSO — synthesis of olefins by the Fischer–Tropsch method;

JGC — Japan Gasoline Corporation;

MCTO — methyl chloride to olefins;

MTE — methanol to ethylene;

MTO — methanol to olefins;

MTP — methanol to propylene;

Non-OCM — non-oxidative coupling of methane;

OCM — oxidative coupling of methane;

OCP — olefin cracking process;

OTP — oxygenate to propylene;

OX–ZEO — oxide–zeolite method;

TIPS RAS — A.V.Topchiev Institute of Petrochemical Synthesis, Russian Academy of Sciences;

UOP — universal oil products.

2. Lower olefins from methane *via* syngas and methanol

Methane processing to lower olefins is a multistage process involving production of syngas (mixture of CO and H_2) followed by the synthesis of methanol, which is then converted to lower olefins either directly or *via* dehydration to dimethyl ether (see Fig. 2).

The conversion of methane to CO and H_2 and the synthesis of methanol are well proven industrial processes.

Methane is processed by the steam,[32,33] oxidative[34,35] or dry[36] reforming reactions on nickel-containing oxide catalysts at high temperatures (750–950 °C).

$$CH_4 + H_2O \longrightarrow CO + 3\,H_2 \quad (1)$$

$$CH_4 + \frac{1}{2}O_2 \longrightarrow CO + 2\,H_2 \quad (2)$$

$$CH_4 + CO_2 \longrightarrow 2\,CO + 2\,H_2 \quad (3)$$

Steam reforming[32,33] or autothermal reforming[37,38] [energy efficient combination of endothermic reaction (1) with exothermic partial oxidation reaction (2)] is most often used. Recently, steam reforming of methane has been carried out in the presence of carbon dioxide,[39] thus combining reactions (1) and (3).

At present, reforming of methane is the main industrial method for activation of thermodynamically stable CH_4 molecule (C–H bond dissociation energy is 439 kJ mol^{-1}).[10] This is a large-scale process basic to the modern production of hydrogen and, to some extent, methanol.

Methanol is synthesized by the reaction

$$CO + 2\,H_2 \longrightarrow MeOH \quad (4)$$

on $Cu/ZnO/Al_2O_3$ catalyst at 270–300 °C and pressures in the range of 5–10 MPa.[40] This is a widely commercialized process with hundreds of production units working worldwide. However, recently, methanol producing facilities have experiencing an overproduction crisis. Attempts to change the situation involve, in particular, starting the construction of large-scale plants for processing of methanol to lower olefins.

Olefins are synthesized from methanol using two methods by the reactions

$$5\,MeOH \longrightarrow C_2H_4 + C_3H_6 + 5\,H_2O \quad (5)$$

$$2\,MeOH \longrightarrow Me_2O + H_2O \quad (6)$$

$$4\,Me_2O \longrightarrow C_2H_4 + 2\,C_3H_6 + 4\,H_2O \quad (7)$$

The first method is direct conversion of methanol on silicoaluminophosphate catalysts at 450–550 °C. Ethylene and propylene are obtained in nearly 1 : 1 ratio in accordance with the stoichiometry of reaction (5) (MTO processes).

The second method involves dehydration of methanol [reaction (6)] followed by conversion of an equilibrium mixture MeOH–DME–H_2O by the reactions (5) and (7) on ZSM-5 zeolites at 430–550 °C with dominant propylene production [in accordance with the stoichiometry of reaction (7)] (MTP processes).

Both types of processes result in polymer-grade ethylene and(or) propylene of purity 99.6%–99.8% in 70%–90% yields.[20,25]

The MTO and MTP processes allow one to combine the olefin and polyolefin markets with the production of methanol, provide flexibility of production and, despite the multistage character, are very attractive to manufacturers. At present, these processes successfully compete (owing to better integration with the available technologies and higher efficiency) with such industrial processes as naphtha pyrolysis and ethane cracking.[41] More than 15 mln tonnes of olefins[1] (~6 mln tonnes of ethylene and ~9 mln tonnes of propylene) are produced yearly from methanol.

High efficiency of methane conversion to lower olefins *via* syngas and methanol is to some extent due to high performance and relatively low raw material consumption per unit of output for the methanol production from syngas.[42] But the key component of success is the well-designed technologies for methanol conversion to lower olefins that have been developed for more than four decades at certain companies and research centres [UOP (Universal Oil Products), Honeywell, Norsk Hydro, INEOS, Total,

Lurgi, Mobil Oil Corporation, Exxon Mobil, DICP, SINOPEC, *etc.*].[7, 25, 43 – 49]

At present, ethylene and propylene are produced from methanol in high yields using shape-selective catalysts (SAPO-34, ZSM-5) and special techniques (recycle of side hydrocarbon products, introduction of additional reaction units, *etc.*).

The MTO process, or direct conversion of methanol to an ethylene/propylene mixture, was designed in the late 20th century as a joint project of UOP (USA) (currently, a subdivision of Honeywell) and Norsk Hydro (Norway) (currently, a subdivision of INEOS, United Kingdom).[43, 44, 50] The process uses silicoaluminophosphate SAPO-34 as catalyst. This is a molecular sieve material with a pore size similar to the size of ethylene and propylene molecules (0.38×0.38 nm). Larger hydrocarbon molecules are retained in the narrow molecular sieve channels. As a consequence, the catalyst exhibits very high shape-selectivity with respect to lower olefins; however, it rapidly cokes. To extend the lifetime of the catalyst before regeneration, a fluidized-bed catalytic reactor is used. The catalyst continuously circulates between the MTO reactor and regenerator where coke is burnt by air. A methanol : water (4 : 1) mixture is fed to the MTO reactor. The temperature and pressure in the reaction zone is maintained at 450 – 550 °C and 0.17 – 0.34 MPa, respectively. Pilot tests of the process (Norway, 1995) on a plant with a daily methanol production capacity of 0.75 tonnes demonstrated a methanol conversion of more than 95% and the following yields of the olefins $C_2^=$, $C_3^=$, $C_4^=$: 40%, 30% and 9%.[43, 44] More recently, the characteristics of the process were improved at Honeywell (UOP) by combining with the Olefin Cracking Process (OCP) for $C_4^=$ olefins. Using catalytic cracking of butenes, the overall single-pass yield of ethylene and propylene was increased by 20% and selectivity to lower olefins was in the range of 85% – 90%.[20, 25] The OCP is carried out in a separate fixed-bed reactor using the technology developed as joint project of Honeywell (UOP) and Atofina. Integration of the MTO process with the OCP technology minimized the yield of the side hydrocarbons C_{4+} and significantly increased the yield of propylene (up to a propylene : ethylene selectivity of 1.3 – 1.8). The MTO – OCP process was fully demonstrated on a Total Petrochemicals pilot plant in Belgium. Its simplified design is presented in Fig. 3. At present, this plant produced polymer-grade ethylene and propylene of 99.8% purity. A large plant for production of lower olefins and polymers from natural gas has been operating in Nigeria (Axinova Polyolefins Ltd) since 2006. The Honeywell UOP company (a subdivision of Honeywell) licenced eight MTO – OCP units in China, some of them (with a total production capacity of more than 3.6 mln tonnes of olefins yearly) are under operation, and a catalysts production line was launched.[51]

Researchers from China developed a number of analogues to the MTO – OCP technology. These are the DMTO/DMTO-II (Dalian Institute of Chemical Physics),[26] SMTO (SINOPEC)[51] and SHMTO (Shenhua Group).[52] All of them differ from one another in certain technological details, being in essence similar to the Honeywell (UOP) technology, *viz.*, utilize SAPO-34 as catalyst, a fluidized-bed reactor and the MTO process integrated with the cracking of C_{4+} hydrocarbons. For instance, the DMTO-II technology differs from MTO – OCP in that (i) the same bifunctional catalyst is used for both methanol conversion to olefins and cracking of hydrocarbons and (ii) the process design is augmented with the recycle of heavier hydrocarbon products C_{4+} to the cracking reactor.[52] A total of 12 MTO installations with a total yearly production capacity of more than 6.5 mln tonnes of olefins started operation in China between 2007 and 2014.[51]

Thus, both the Honeywell (UOP) process and the Chinese MTO technologies are fully developed and proven industrial processes. They enable production of lower olefin mixtures at propylene : ethylene mass ratios from 0.7 to 1.8,

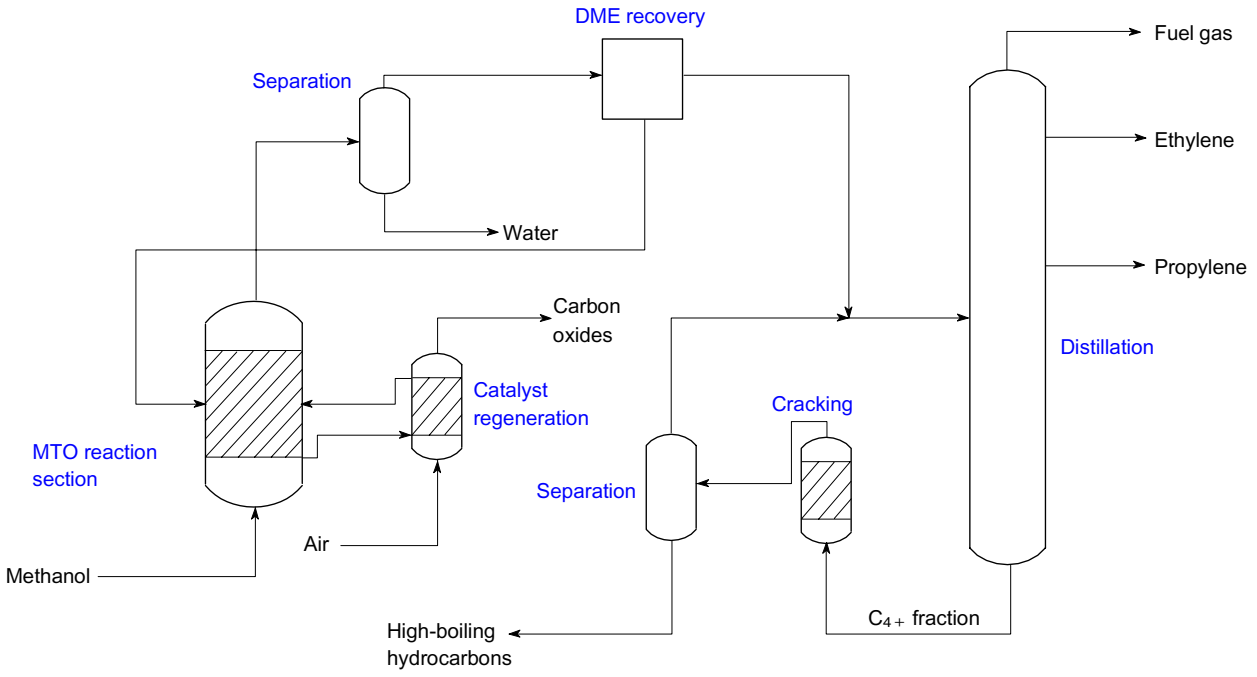


Figure 3. Simplified flow diagram of MTO – OCP process [Honeywell (UOP), INEOS, Total].[42]

which meets the demands of the olefin market (propylene : ethylene mass ratio should be at least 0.6).[8, 53]

At the same time, owing to increasing 'propylene gap' in the world olefin sector[8, 53] there has been demand for processes aimed at producing propylene as target product (Methanol to Propylene, MTP) rather than a mixture of olefins.

German company Lurgi GmbH leads in production of propylene from methanol (62% of world production). Noteworthy is that large-scale production of methanol is combined with the production of propylene and premium gasoline.[45, 46] A number of commercial units owned by Lurgi with a total yearly production capacity of more than 2 mln tonnes of olefin are under operation in China[52] and in Trinidad and Tobago; a propylene production plant with a yearly production capacity of 100 thousand tonnes is under design in Iran (Bandar Imam Khomeini Methanol Plant; plant owner: Fanavaran Petrochemical Co.). The Lurgi process involves the synthesis of propylene *via* dehydration of methanol.[45, 54] A simplified design of the Lurgi MTP process is presented in Fig. 4. First, methanol is converted to equilibrium mixture of DME, methanol and water vapours in an adiabatic reactor on alumina at ~380 °C. The mixture is fed into a cascade of fixed-bed shaft reactors (modified zeolite ZSM-5 as catalyst, channel size 0.52 × 0.56 nm) and converted to a mixture of hydrocarbons with high content of propylene (20 vol.% – 50 vol.%) at 430–450 °C and a pressure of 0.35 MPa. Propylene is separated from other gaseous products, gasoline is separated from liquid reaction components, while the side hydrocarbon products ($C_2^=$ olefins and $C_4^=$ and C_5–C_8 hydrocarbons) are returned to the olefin synthesis stage. Recycle of the side products significantly increases the yield of the target product. The yield of propylene in the MTP process can be as high as 65%–70% at a methanol conversion of more than 99%. The process affords propylene as the major product and premium gasoline as a by-product. The catalyst lifetime is more than 700 h, being due to spatial separation of the reaction section, *viz.*, three MTP reactors are connected in parallel, one of them being used for catalyst regeneration (air is supplied for coke oxidation).

Yet another process for production of propylene *via* dehydration of methanol (Dominant Technology for the Propylene production, DTP) was developed in Japan as joint project of JGC Corporation and Mitsubishi Chemical Corporation.[6] A demonstration plant has two reaction units (a reactor for methanol dehydration and a DTP reactor for the synthesis of olefins) and a catalyst regenerator. Olefins C_{4+} from a naphtha cracking facility are additionally fed into the DTP reactor. High yield of propylene (>70%) is due to recycle of hydrocarbon products (C_1–C_2 and C_4–C_6) and high selectivity of the ZSM-5-based zeolite catalyst in the MTP and olefin disproportionation reactions. Gasoline is obtained as a by-product in 16% yield. Currently, the DTP technology is under development at the Mitsubishi Chemical's Mizushima Demonstration Plant.

Van Dijk Technologies (USA) patented a Methanol-to-Ethylene (MTE) process that is similar to the Lurgi MTP process, involves partial conversion of methanol to DME in an adiabatic reactor and multistage synthesis of olefins from a mixture of DME and methanol, and is aimed at producing ethylene rather than propylene as target.[55] Ethylene is formed from a DME + methanol mixture diluted with steam over a fixed bed of the H-SAPO-34 catalyst. The partial pressure of the DME + methanol mixture in all reactors in a cascade is maintained low (about 0.003–0.007 MPa); this allows one to suppress undesired conversion of ethylene to propylene. Using a three-reactor cascade for the synthesis of olefins, the conversion of methanol is more than 70% and the ethylene selectivity is 70%.

Thus, various processes have been proposed for production of lower olefins from methanol. They differ in catalysts and design details. Certain processes are aimed to produce a mixture of ethylene and propylene (MTO, MTO–OCP,[43, 44] DMTO, SMTO[25]), while other afford only propylene (MTP,[45, 46] DTP[6]) or ethylene (MTE[55]). There are two well-developed methods for processing of methanol to

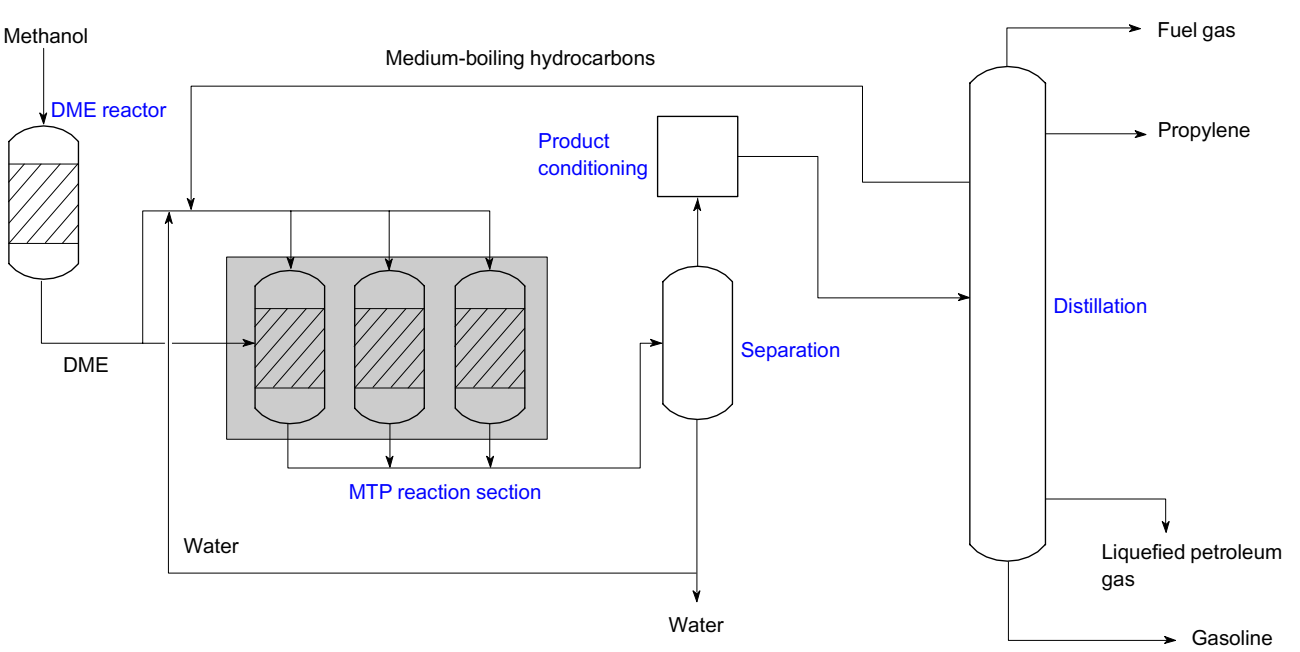


Figure 4. Simplified flow diagram of MTP process (Lurgi).[42]

olefins, *viz*., direct conversion of the alcohol and *via* dehydration of methanol to dimethyl ether (see Fig. 2).

Although certain processes for production of olefins from methanol have been industrialized or are close to industrialization, studies in this field continue. Recently, a number of fundamentally different MTP processes without preliminary dehydration of the alcohol were proposed. Two of them are developed at ExxonMobil Corp. (USA). One process uses an adiabatic fixed-bed reactor and a gallium-containing ZSM-5 zeolite,[49] while the other utilizes a fluidized-bed catalytic reactor and a mixed molecular sieve catalyst SAPO-34/SAPO-18.[48] In both cases olefins are synthesized at 450 – 500 °C and a methanol conversion of >98%. The single-pass yield of propylene reaches 43% (Ref. 49) – 50% (Ref. 50). The total $C_3^= + C_2^=$ selectivity is 56% (Ref. 50) – 73% (Ref. 49) and the $C_3^= : C_2^=$ ratio in the product varies from 1.4 (Ref. 49) to 8 – 9.[50]

The Fluidized Methanol-to-Propylene (FMTP) process proposed at Tsinghua University (China) is also based on the SAPO-18/SAPO-34 catalyst.[25] It was declared that mixed silicoaluminophosphates exhibit higher $C_3^=$ selectivity compared to SAPO-34 and can limit the formation of the C_{4+} compounds and thus to reduce the amount of the side products to be recycled. The flow diagram of the FMTP process includes two fluidized-bed catalytic reactors connected in series. One reactor is utilized to convert methanol to lower olefins, while the other one is necessary for converting ethylene and butenes to propylene. The reaction units have unique gas – solid counterflow configurations that facilitate controlling the reaction temperature and suppress the secondary and side reactions and thus increase the selectivity to the target product. The technology enables fine tuning of the ethylene : propylene ratio in the product in the range of 0.02 – 0.85, as well as production of pure propylene. The single-pass yield of propylene can be higher than 67% at a propylene : ethylene ratio of 2 and a methanol conversion of 99.5%.[56] A demonstration plant with a yearly production capacity of 30 000 tonnes of propylene started operation in 2009. Recently, a production plant with a yearly production capacity of 200 000 tonnes of propylene was constructed.

Yet another example of a method for direct conversion of methanol to propylene is provided by the Honeywell (UOP) Oxygenate to Propylene (OTP) process based on the moving bed technology.[47] Methanol diluted with steam is converted to olefins on the SAPO-34/ZSM-5 composite catalyst. The catalyst layer continuously circulates through a cascade including at least three adiabatic MTP reactors connected in series and a regenerator. The reaction product arrives at the separation unit, propylene and gasoline hydrocarbons are separated while the remaining components of the reaction flow (water, ethylene, C_{4+} olefins) are returned to the first MTP reactor. The process provides a high yield of propylene (>71%) and stable operation of the catalyst (catalyst lifetime before regeneration from coke is 200 h). Gasoline is obtained as a by-product product in yield >19%.

Despite the announced high performance and other parameters, various methods for direct conversion of methanol to propylene have not been industrialized so far. This is, in particular, due to complexity of the flow diagrams of the new MTP processes, although the methanol dehydration step is excluded.

Concluding this Section, the flow diagrams of the modern processes for production of lower olefins from methanol are rather complicated and imperfection of catalysts is to some extent compensated by engineering means. Further improvement of the efficiency of the MTO and MTP processes requires new catalysts with higher stability and selectivity, especially with respect to propylene formation. The development of such catalysts has been the focus of activity in many research centres worldwide[18,19] in addition to studies on the mechanism of methanol conversion to hydrocarbons[21,24] and elucidation of the reasons for coking and deactivation of zeolite catalysts.[57 – 61]

3. Lower olefins from methane *via* syngas and dimethyl ether

A new three-stage process for advanced processing of natural gas to lower olefins has been developed. Like the 'methanol' processes, the new method involves methane conversion to syngas, but proceeds *via* its conversion to dimethyl ether followed by DME conversion to ethylene or propylene:

$$\text{methane} \longrightarrow \text{syngas} \longrightarrow \text{DME} \longrightarrow \text{lower olefins}$$

This route from methane to ethylene(propylene) *via* dimethyl ether offers some advantages over the 'methanol' methods. For instance, more favourable thermodynamics allows one to synthesize DME at lower pressure compared to the synthesis of methanol and reach a higher single-pass conversion of syngas.[62] This leads to energy and capital savings and allows one to improve the utilization efficiency of natural gas and to reduce the production cost.[63] Other advantages are as follows:

— reduction of thermal load in (or lower exothermicity of) the synthesis of olefins from DME due to elimination of exothermic methanol dehydration reaction;[64]

— DME is more reactive and selective than methanol in the synthesis of olefins;[24] and

— the possibility to produce not only ethylene and propylene, but also dimethyl ether, a new valuable product on the chemical and fuel markets (the demand for DME has increased by more than 400 times since 2000).[65]

Dimethyl ether is treated as alternative green domestic, transportation and turbine fuel, intermediate feedstock in production of synthetic premium gasoline, polymeric products and organic chemicals. A number of large-scale plants for production of DME from syngas operate in China, Japan, in the Far East of the Russian Federation (development companies are Haldor Topsøe, KOGAS and JGC). Integration of the new production flow diagrams for direct synthesis of DME from syngas into the available olefin (polyolefin) production cycle will expand the range of products, minimize the production risks and create an economic 'safety net' for complex large-scale production.

Methods for production of lower olefins *via* synthesis of DME from syngas are developed in Japan (at JGC Corporation),[66] in China (at Dalian Institute of Chemical Physics, DICP)[67] and in the Russian Federation at TIPS RAS[68 – 71] (Table 1).

Syngas preliminarily obtained by reforming of methane is converted to DME by the reaction

$$3\,CO + 3\,H_2 \longrightarrow Me_2O + CO_2 \qquad (8)$$

on bifunctional catalysts containing catalytic sites for the synthesis of methanol and dehydration of alcohol. Olefins

Table 1. Processes for natural gas conversion to lower olefins *via* direct conversion of syngas to dimethyl ether.

Parameters and characteristics	Process (development company)		
	JGC (see [a]) Corporation [66]	DICP (see [a]) [67]	TIPS RAS (see [a]) [68 – 71]
	Syngas conversion to DME (as mixture with methanol)		
Catalyst	$CuO-ZnO/Al_2O_3 + Al_2O_3$	$CuO-ZnO/Al_2O_3$ + zeolite	$CuO-ZnO-Cr_2O_3-Al_2O_3$
Temperature /°C	210 – 300	265	260
Weight hourly space velocity /h^{-1}	–	1000	5500
Pressure /MPa	3 – 15	4	11
CO conversion (%)	to 90	to 90	88
DME (+methanol) selectivity (%)	99	99	> 70
	DME conversion to olefins		
Active component of catalyst	SAPO-34	SAPO-34	ZSM-5
Temperature /°C	500	450	340
Pressure /MPa	0.15	0.1	0.1
Reactor type	FBCR [b]	FBCR [b]	AFBCR [b]
Catalyst recovery	Continuous	Continuous	Periodic
Raw material — DME : methanol (mass %)	35 : 65 (see [c])	50 : 50 (see [c])	100 : 0 (see [d])
Weight hourly space velocity /h^{-1}	3000	2000	2000
DME conversion to methanol (%)	97	100	96
$C_2^= - C_4^=$ selectivity (%)	89	82	90
Yield of olefins (%)	87	82	87
Catalyst lifetime before recovery for decoking /h	1 – 2	1 – 2	700
Reaction product composition (%):			
ethylene	33	40	32
propylene	47	34	48
butenes	9	8	10
methane	1.5	–	0.5
alkanes C_2-C_5	9.5	–	9.5

[a] JGC stands for Japan Gasoline Corporation and TIPS RAS stands for A.V.Topchiev Institute of Petrochemical Synthesis, Russian Academy of Sciences.
[b] FBCR stands for fluidized-bed catalytic reactor and AFBCR stands for adiabatic fixed-bed catalytic reactor.
[c] Substrate is diluted with water.
[d] Substrate is diluted with syngas.

are synthesized from DME by reaction (7) on zeolites or silicoaluminophosphates. Carbon dioxide, a side product of DME synthesis, is returned in the stage of methane reforming,[72] which improves the efficiency of utilization of carbon-containing raw material up to more than 80%.

The processes proposed mainly differ in methods for the synthesis of olefins. Chemists from Japan and China obtain olefins from a DME + methanol mixture on SAPO-34 at 450 – 500 °C,[66, 67] whereas researchers from the TIPS RAS convert DME to olefins on ZSM-5 at 320 – 360 °C using pure dimethyl ether.[70, 71] In all cases the yield of lower olefins is in the range of 82% – 87% and 74% – 80% of these are ethylene and propylene. The efficiency of olefin synthesis from DME is so high that the single-pass characteristics attained without using any other design features are higher than those of industrial methanol processes having complicated flow diagrams (MTO – OCP, MTP-Lurgi, *etc*.). In the future, processes involving DME may appear to be competitive with the commercial methanol methods.

However, at present production of lower olefins *via* DME is in the early stage of industrialization. Commercialization of the processes proposed by researchers from Japan and China is hampered by rapid coking and deactivation of the SAPO-34 catalyst. The process proposed at the TIPS RAS is under development on a pilot plant at the Elektrogorsk Institute of Petroleum Processing (Moscow Region, Russia). The yearly production capacity of the plant is 4 tonnes of olefins. The results of pilot tests suggest a high promise of the process.

All known methods for methane conversion to ethylene (propylene) *via* direct conversion of syngas to dimethyl ether have a common drawback, *viz*., a poorly elaborated synthesis of lower olefins from DME (Dimethyl Ether to Olefins, DTO).

Chemists study specific features of the mechanism of DME conversion to hydrocarbons [22, 24] and design novel modifications of catalysts to improve the efficiency of the DTO reaction. The possibility to use concentrated DME would make the DTO reaction much more efficient due to reduced volume of the reaction section and simplified procedure for product isolation and make the DTO step more technologically and economically attractive.

Recently, interest in the DTO reaction increased considerably. There has been high research activity in many research centres (Tsinghua University, Qingdao University, Osaka University, Tohoku University, Iran Petroleum University of Technology, Korea Institute of Energy Research, SABIC, University of the Basque Country, *etc.*).

It was proposed [64] to carry out the DTO reaction using neat DME in the Berty reactor developed at Chemical Reactor Engineering Centre (Canada). This is a gradientless reactor with intense internal circulation. The reaction flow continuously circulates by means of an impeller running at 1500 rpm through a fixed bed of the catalyst held in a special basket. This reactor makes it possible to carry out the DTO reaction on HZSM-5 zeolite ($SiO_2 : Al_2O_3 = 280$) at temperatures below 450 °C with a stable catalyst activity and to obtain the product with high content of propylene ($C_3^= : C_2^= = 1.7-4.2$) at DME conversions to 60%. However, the yield of the lower olefins $C_2^= - C_4^=$ still remains rather low (~30%) at a selectivity of 50% – 60%.

Researchers from TIPS RAS reported high conversion of concentrated DME in the synthesis of olefins on nanosized Mg-HZSM-5 zeolites (crystallite size ~100 nm) dispersed in silicone oil.[73] The reaction was carried out in a gradientless slurry reactor at low DME weight hourly space velocity ($W_{DME} = 0.7\ h^{-1}$) at 320 °C under atmospheric pressure. Olefins were synthesized from DME in the three-phase system gaseous substrate – solid ultradispersed heterogeneous catalyst – liquid reaction medium in the steady-state mode. The catalyst was maintained in the state of ultradispersed suspension [74] and its parameters and characteristics approached those of homogeneous systems that exhibit the highest catalytic activity. Owing to rapid continuous removal of reaction heat and reaction products from catalyst grains to the reaction medium the efficiency of the olefin synthesis was almost independent of the DME concentration (in the range of 20 vol.% – 90 vol.%). Reactions using both 50%-DME and 90%-DME afforded ethylene as the major product, the conversions in the range of 84% – 87% and the selectivity with respect to lower olefins was 46% to 55%. High values of parameters were attained using the innovative three-phase design of the DTO reaction, which combines the advantages of heterogeneous process (continuity and ease of separation of reaction product from the catalyst) and homogeneous catalysis (high activity and selectivity of the catalyst).

4. Catalysts for the synthesis of lower olefins from methanol and dimethyl ether

At presence, there are two industrial processes for production of olefins from syngas *via* methanol:

— using ZSM-5 zeolites as catalysts;[46] and

— using SAPO-34 molecular sieves as catalysts.[44]

Publications on the synthesis of lower olefins from syngas *via* DME or concerning the development of the DTO stage are few compared to the literature on the MTO processes.

At the same time, the design of catalysts for the DTO reaction deserves particular importance because DME is more suitable for the synthesis of olefins than MeOH from the standpoint of chemical properties.[75 – 78] Dimethyl ether is a stronger methylating agent than methanol,[75, 76] which allows one to carry out the DTO reaction as rather fast process even on catalysts of low acidity (*e.g.*, zeolites with a high silica modulus of up to Si : Al = 560).[79] In addition, DME is less reactive in the undesired hydrogen transfer reactions [24, 77, 78] resulting in the formation of carbonaceous deposits, deactivation of the catalyst in the course of DTO reaction proceeds much slower than in the reaction with methanol.[24, 80]

It should be noted that diffusion of DME into pores of the molecular sieve catalyst can be complicated by coordination of bulky DME molecule to active sites. This is the reason for pronounced dependence of the rate of DTO reaction and, often, the selectivity of olefin formation on the characteristics of the porous system of the molecular sieve catalyst (topology of the crystal lattice,[71, 81] micro-/mesopore volume ratio in the molecular sieve framework,[81, 82] micropore size [83]). Indeed, the use of mesoporous high-silica ZSM-5 zeolites with MFI topology causes almost no diffusion constraints and reactions with DME are characterized by conversions higher than 90% (Refs 22, 83, 84) and selectivity with respect to lower olefins higher than 80%.[71] When using EU-1 zeolite, which has the same acidic characteristics and micropore size but different topology (EUO), the DTO reaction proceeds much slower (conversion is 37%).[81, 82]

Recently, olefins have been synthesized from dimethyl ether on silicoaluminophosphate molecular sieves SAPO-34,[80, 85 – 87] SAPO-18,[88] SAPO-5,[24] SAPO-18/34 (Refs 89, 90) and on various zeolites including ZSM-5,[83, 84] SSZ-24,[24] mordenite,[91] EU-1,[81, 82] ZSM-34,[92] *etc*. Like in the case of the reaction with methanol, most studies were carried out using SAPO-34 and ZSM-5.

4.1. Catalysts based on SAPO-34

Molecular sieve catalysts SAPO-34 demonstrated the highest selectivity in the reaction with methanol.

Catalysts based on SAPO-34 are of interest to industry for their high shape-selectivity to ethylene and propylene. The CHA-type crystal structure (narrow channels and small windows 0.38×0.38 nm in size, formed by eight oxygen atoms associated with six Si – Al – P tetrahedra) [93] of the SAPO-34 molecular sieve is such that only small olefin molecules can be sieved. However, this does not exclude chemical transformations of larger hydrocarbon molecules retained in the narrow channels of the molecular sieve and leads to formation of carbonaceous deposits in the catalyst pores.[94] Coke species cause pore blockage of the molecular sieve, thus making its active sites inaccessible,[57] and the catalyst rapidly deactivates.

Recently,[95, 96] it was established that deactivation of the catalyst is due to coking-induced intra-diffusion constraints rather than coking *per se*. These constraints complicate diffusion of reactants and reaction products and thus have a negative impact on not only the lifetime of the catalyst, but also the selectivity.[96] The larger the crystallites and the higher the density of acidic sites the more severe the constraints.[96] In this connection it is a decrease in the crystal size [87, 97] and variation of acidity [97] that underlie a recently used strategy for improving the catalytic properties of SAPO-34 in the MTO reaction.[87, 98 – 100]

The use of catalytic systems with SAPO-34 nanocrystallites (25–75 nm in size) instead of an industrial catalyst (crystals 2–4 μm in size)[101] leads to an increase in the catalyst lifetime (by 10 to 15 times) and in the selectivity to lower olefins as well as makes propylene the major product of the MTO reaction.[87, 102]

The proportion of strong acidic sites in the SAPO-34 lattice can, in particular, be decreased by introducing transition metals into the molecular sieve framework. It was shown[97] that nanosized SAPO-34 modified by adding Co to give Co–SAPO-34 exhibits a 50-fold increase in lifetime and the selectivity of the catalyst to ethylene and propylene becomes as high as 90%.

Modification of the CHA-type crystal structure is also efficient. Fabrication of mixed catalysts composed of CHA-type (SAPO-34) crystalline framework and AEI-type (SAPO-18)[48, 81] or MFI-type (ZSM-5)[82, 83] molecular sieves leads to partial structural changes and to a decrease in the proportion of strong acidic sites. This improves the properties of the catalyst, its stability in the MTO reaction and the propylene selectivity.

Composite catalysts SAPO-34/SAPO-18 are of considerable interest.[48, 103, 104] Both silicoaluminophosphate sieves, SAPO-18 and SAPO-34, have similar crystal lattices with same-size pores (0.38×0.38 nm),[93] but the AEI cage is slightly wider than the CHA one (1.16 *vs.* 0.94 nm, respectively).[104] Therefore, the mixed SAPO-18/SAPO-34 molecular sieve catalyst is characterized by higher propylene selectivity and lower selectivity to alkanes and C_{4+} hydrocarbons.[48]

The situation with the SAPO-34/ZSM-5 composite catalysts is more complicated[105, 106] since their selectivity to lower olefins is lower than that of SAPO-34 (many alkanes). Nevertheless, mixed catalytic systems composed of CHA-type (SAPO-34) and MFI-type (ZSM-5) frameworks are very stable (catalyst lifetime is longer than 100 h).[106] However, the catalytic properties of such composites in the MTP reactions depend strongly on the catalyst preparation procedure and on the mass ratio of the components.[105, 106]

Composite mixed molecular sieves SAPO-34/SAPO-18 and SAPO-34/ZSM-5 are used as catalysts of new processes of direct conversion of methanol to propylene (FMTP,[25] OTP[47]). However, the single-pass yield of propylene over such systems is at most 40%, and there is a strong competition between the systems in question and catalysts based on high-silica zeolite ZSM-5 that exhibit higher propylene selectivity in the MTO reaction.

In contrast to the MTO reaction, carrying out the DTO reaction on narrow-pore molecular sieves SAPO-34 and SAPO-18 is problematic owing to bulkiness of DME molecule.[80, 85, 86, 88, 92] Recently, a discussion began in the literature[80, 85, 86] of suitability of utilizing SAPO-34 in the DTO reaction, although it is these catalysts that are used for the synthesis of olefins from DME in the JGC and DICP processes.[66, 67]

The behaviour of DME and methanol in the synthesis of olefins on SAPO-34 was compared.[80, 85, 86, 107] It was established that the initial rate of the reaction with DME is higher than with methanol.[85] The DTO process affords almost no aromatic hydrocarbons,[86] but the reaction products can contain methane and methanol due to specific features of DME coordination to the acidic sites.[80] It is believed[23] that hypothetical primary product with C–C bond (2-methoxyethanol) is converted to propylene; indeed, the authors of most studies reported dominant formation of propylene among hydrocarbons in the initial stage of the DTO reaction on SAPO-34.[86, 107, 108] However, the development of the process causes the distribution of olefins to change and become nearly identical to that observed in the reaction with methanol; the reaction products can contain large amounts of CH_4 (10%–20%) and MeOH (2%–6%).[80] Thus, the synthesis of olefins from DME on SAPO-34 under steady-state conditions is less favourable than the MTO reaction from the standpoint of reaction rate and selectivity.

Meanwhile, the silicoaluminophosphate catalyst is more stable in the DTO reaction than in the MTO process.[80, 85, 107] This gives a strong impetus to the develop-

Table 2. Characteristics of SAPO-34- and SAPO-18-based catalysts of DTO reaction.

Catalyst	DME concentration[a] (vol.%)	T/°C	Time /h	DME conversion (%)	Selectivity to olefins (%)			Catalyst lifetime /h	Ref.
					$C_2^=$	$C_3^=$	$\sum C_2^= - C_4^=$		
SAPO-34	98.5	460	7	~100	51	24	79	7	80
SAPO-34	25	400	1	95	29	41	90	1–2	108
	25	400	3	12	40	36	90	1–2	108
SAPO-34/α-Al_2O_3	25	400	1	99.5	16	31	72	4	108
	25	400	3	99.5	32	43	91	4	108
SAPO-34/ZrO_2	25	400	1	100	15	30	68	6	108
	25	400	3	100	39	42	92	6	108
SAPO-18 (hydrothermal method)	100	400	1	98	18	40	78	1–2	88
	100	400	3	50	17	38	76	1–2	88
SAPO-18 (dry gel method)	100	400	1	100	22	41	82	3–4	88
	100	400	3	95	21	42	81	3–4	88
SAPO-34/SAPO-18	100	400	1	100	49	34	89	–	89, 90
	100	400	3	100	48	33	88.5	–	89, 90
SAPO-34/bentonite	100	350	0.5	2	18	32	63	–	83
SAPO-18/bentonite	100	350	0.5	5	21	50	87	–	83

[a] DME diluted with inert gas (nitrogen or helium).

ment of novel modifications of SAPO-based catalysts for the synthesis of olefins from DME (Table 2).[85,86,108] By varying the process conditions and the composition of the catalytic system researchers try to reduce the proportion of methanol and methane formed from DME, to increase the catalyst lifetime and propylene selectivity and to stabilize the composition of reaction products formed throughout the process.

It was shown[83,88–90,108] that the rate of MeOH and CH_4 formation in the DTO reaction decreases as temperature decreases and DME is diluted with inert gas. Almost no methane and methanol is formed at 400 °C upon dilution of DME with nitrogen to 25 vol.%, while the $C_2^=-C_4^=$ olefins are obtained from DME on SAPO-34 at a selectivity up to 90% at an initial DME conversion up to 95% (the major side products include C_2-C_4 alkanes and heavier linear C_{5+} hydrocarbons).[86]

The catalyst lifetime was increased[108] by 2 to 5 times using the SAPO-34/Al_2O_3 or SAPO-34/ZrO_2 composite systems; however, the DTO process on these and SAPO-34 catalysts cannot be treated as steady-state one because the selectivity with respect to olefins varies with time.

A stable composition of reaction products was obtained[88–90] when the DTO reaction was carried out on the SAPO-18 silicoaluminophosphate[88] and on the (SAPO-34/SAPO-18) mixed catalyst.[89,90] At 400 °C, the major olefin was propylene in the former and ethylene in the latter case. By varying the composition of the silicoaluminophosphate one can vary the $C_3^=:C_2^=$ ratio from 0.7 to 2. Having reduced the temperature to 350 °C, the $C_3^=:C_2^=$ ratio for the process on SAPO-18 was increased to 2.4 and propylene was obtained with a selectivity up to 50%; however, the catalyst activity at this temperature was very low and the yield of olefins was at most 3%.

The catalytic properties of two silicoaluminophosphates, SAPO-34 and SAPO-18, and mesoporous ZSM-5 zeolites in the DTO reaction at 350 °C and 400 °C were compared.[83,84] The silicoaluminophosphates had better shape selectivity than zeolites, but the latter were much more active and stable; as the temperature decreased, the differences were more pronounced. At temperatures below 400 °C, the yield of ethylene and propylene on SAPO-34 and SAPO-18 was ten times lower while the catalyst lifetime was 10 to 60 times shorter than in the reaction on ZSM-5. Thus, silicoaluminophosphate catalysts seem not to be the best choice for the synthesis of olefins from DME.

4.2. Catalysts based on ZSM-5 zeolites

At present, the ZSM-5 zeolites are considered as the most promising catalysts of the DTO reaction.[83,84] The pore size in the crystal lattice of ZSM-5 presents no steric hindrances to coordination of DME molecule to acidic sites, and the synthesis of olefins from dimethyl ether on ZSM-5 proceeds 16 to 20 times faster than from methanol.[24,84] Also, the active sites are deactivated slower,[24] which leads to higher yield and improved distribution of reaction products.

The synthesis of olefins from DME on ZSM-5-type zeolites is carried out at 320–450 °C, usually, at a reduced DME pressure to prevent secondary reactions of lower olefins (Table 3). In most cases, the zeolites are modified with nonmetals (Si[109] and P[110]) or metals (Ca,[111] Mg,[112–115] Rh,[71] Zn,[116] Zr,[116] La,[116] Co,[116] and Ti[117]). Other modification patterns are as follows: metal–nonmetal (Zr–P,[110] Ti–S[117]), two metals (Zn–Zr,[116] La–Zr,[116–118] Mg–La,[119] Mg–Zr[119]), three metals (Mg–La–Zr,[119] Rh–La–Zr[71]), two metals and a nonmetal (Rh–chitosan–Mg[120]). The reaction is studied on powdered and pelleted modified zeolites,[109–112] on composite extrudates prepared by mixing zeolites with a binder (usually, γ-Al_2O_3),[113–119] and even on ultradispersed zeolite-containing suspensions (Mg—ZSM-5 in silicone oil).[115]

Modification of ZSM-5 zeolite was also used to prepare efficient catalysts of the MTP reaction. The HZSM-5 zeolite was modified with phosphorus,[121–123] silicon,[124,125] alkali and alkaline-earth metals (Cs,[121] Ca,[126] Mg[126,127]), as well as with manganese,[128,129] bismuth,[130,131] antimony[130] and lead oxides.[130] Doubly modified (Mn–Fe, Mn–Cr, Mn–Ce) systems based on the HZSM-5 zeolite were also reported.[129]

The influence of the modifier nature, acidity and magnitude of the silica modulus of the HZSM-5 zeolite on characteristics of the DTO and MTP reactions was thoroughly considered in a review.[19]

Dilution of hydrocarbon raw material with steam has strong effect on the catalyst stability in the DTO reaction. For instance, the reaction on HZSM-5 zeolite (Si : Al = 560) using DME diluted with steam (10%) afforded propylene in 57% yield at 100% DME conversion and minimum formation of coke species. The catalyst retained its catalytic properties for at least 40 h, probably, due to more intense desorption of olefins which precluded the formation of side products.[124]

A stabilizing effect of steam on the course of olefin synthesis from DME on catalysts containing the ZSM-5 zeolites (Si : Al = 15 and 140) in the H-form or modified with metals (Mg, La–Zr) was also reported.[118,132–135] It was established[133] that the reaction using DME diluted with steam on the HZSM-5/γ-Al_2O_3 catalyst is accompanied by much slower coke formation compared to the reaction using nitrogen as diluting agent. The stabilizing effect of steam on the DTO process was explained by reduction of the partial pressure of reactants, by competition between water and coke precursors for acidic sites and by diffusion of coke precursors from the zeolite micropores to the substrate mesopores.[133–135] It should be noted that the stabilizing effect of H_2O added to hydrocarbon raw material is more pronounced for the DTO reaction[133] than for the industrial MTO process (Honeywell (UOP)/Total) where the substrate is also diluted with steam.[20] Therefore, the synthesis of lower olefins from DME diluted with steam seems to be a very promising strategy.[133–135]

4.3. Catalysts based on nanosized ZSM-5 zeolites

At present, considerable attention is paid to the design of nanosized ZSM-5-based zeolite catalysts of the MTP and DTO reactions. Nanosized zeolites offer such advantages as large specific surface area and ready accessibility of active sites. These features underlie high activity, better operating characteristics and longer lifetime of such catalysts.[136–138]

Two main strategies for the preparation of nanosized zeolites include

— reduction of the zeolite crystal size to nanometre scale, and

— creation of secondary pores larger than 2 nm in diameter in the crystal lattice to form a hierarchical porous system with transport meso(macro)pores in order to make active sites more accessible and facilitate adsorption processes and catalytic reactions.

Nanosized zeolites are mainly prepared using synthetic methods, which enables not only the growth of nanocrys-

Table 3. Characteristics of ZSM-5-type zeolite catalysts of DME conversion to lower olefins (under partial vacuum with respect to DME).[a]

Catalyst	SiO_2 : Al_2O_3	DME concentration (vol.%)	T/°C	DME conversion (%)	Selectivity to olefins (%)			Ref.
					$C_2^=$	$C_3^=$	$\sum C_2^= - C_4^=$	
Si – HZSM-5 (see [b])	39	10	400	100	8	13	–	109
Zr – P – HZSM-5	84	17	450	100	5	45	65	110
Ca – HZSM-5	23	7	450	> 97	10	45	57	111
Ca – HZSM-5	23	7	400	> 95	7	30	50	111
Ca – HZSM-5	23	7	350	< 60	5	25	40	111
Mg – HZSM-5	33	10	320	85 – 90	33	26	74	112
HZSM-5/γ-Al_2O_3	37	20	340	94	22	23	56	113
Rh – HZSM-5/γ-Al_2O_3	37	10	340	100	24	19	50	71
Mg – HZSM-5/γ-Al_2O_3	37	20	340	86	36	22	67	113, 114
Mg – HZSM-5/γ-Al_2O_3	37	10	450	100	15	35.5	68	113
Zn – HZSM-5/γ-Al_2O_3	37	20	360	90	23	41	79	116
Zr – HZSM-5/γ-Al_2O_3	37	20	360	96	37	33	85	116
La – HZSM-5/γ-Al_2O_3	37	20	360	96	23	32	68	116
Co – HZSM-5/γ-Al_2O_3	37	20	360	89	20	14	46	116
Ti – HZSM-5/ γ-Al_2O_3	37	10	320	70	13	18	43	117
Ti – S – HZSM-5/γ-Al_2O_3	37	10	320	90	25	33	73	117
Zn – Zr – HZSM-5/γ-Al_2O_3	37	20	360	96	29	42	83	116
La – Zr – HZSM-5/γ-Al_2O_3	37	20	360	98	29	49	89	116
La – Zr – HZSM-5/γ-Al_2O_3	37	20	340	70	26	44	77	118
Mg – La – HZSM-5/γ-Al_2O_3	37	10	320	84	23	27	73	119
Mg – Zr – HZSM-5/γ-Al_2O_3	37	10	320	54	20	35	66	119
Mg – La – Zr – HZSM-5/γ-Al_2O_3	37	10	320	77	23	28	73	119
Rh – La – Zr – HZSM-5/γ-Al_2O_3	37	10 (see [c])	340	96	32	48	90	71
Rh – chitosan/Mg – HZSM-5	33	10	320	99	38	26	79	120
Mg – HZSM-5/Syltherm 800	80	10	330	94	9	46	69	115

[a] DME is diluted with inert gas (nitrogen or helium), the total pressure is 0.1 MPa; $W_{DME} = 1 - 3\ h^{-1}$.
[b] With 1,4-bis(hydroxydimethylsilyl)benzene as silylating agent and aromatic hydrocarbons as major reaction products.
[c] Diluted with a $CO : H_2 = 1 : 1$ mixture.

tallites, but also targeted modification of the porous system of the zeolite and even change of the chemical composition of its framework. Recently, various methods for the synthesis of ZSM-5 zeolite analogues with modified acidic and porous characteristics of the crystal lattice have been developed [138 – 154] and new efficient catalysts of the MTP reaction have been designed (Table 4).[49, 105, 130, 137, 141, 142, 144 – 157]

The development of efficient nanosized zeolite catalyst became possible owing to the use of modern methods of nanotechnology that made it possible to fabricate molecular sieves with shortened channels and micro(meso)porous structure. It is these methods that were used to create efficient nanosized catalytic systems with hierarchical structure (in fact, with new design), namely, spherical aggregates of ZSM-5 nanocrystals,[150] nanosheets,[153, 154] and nanowhiskers [157] (Fig. 5 *a – d*).

Small zeolite crystals are usually formed if the nucleation rate is higher than the crystallite growth rate. The zeolite framework can be composed by surrounding positively charged species (*e.g.*, alkali metal cations) or organic molecules acting as structure-forming agents (templates) with AlO_4^{-5} and SiO_4^{-4} tetrahedra. The size, shape and nature of the templates influence the formation of the zeolite phase.

The ZSM-5 zeolite crystals 130 – 230 nm in size were for the first time synthesized by Persson *et al.*[158] at a low temperature using tetrapropylammonium chloride as the template. Since then, various research groups attempted to reduce the zeolite crystal size, to increase the crystallization rate and to shorten the crystallization time.[159 – 162]

Methods for preparation of ZSM-5 nanocrystallites using various organic templates were patented.[160 – 164] Most often, ZSM-5 nanocrystallites are synthesized from transparent solutions using tetrapropylammonium hydroxide (TPAOH). This template allows one to synthesize ZSM-5 nanocrystallites from 1 to 100 nm in size.[162, 163] It was shown [158] that a decrease in the TPAOH content in the

Table 4. Characteristics of new ZSM-5-type zeolite catalysts of MTP reaction [a] obtained by different synthetic methods.

Catalyst	Crystal size	Morphological features	Synthesis details	Selectivity to olefins (%)			Catalyst lifetime /h	Ref.
				$\sum C_2^= - C_4^=$	$C_3^=$	$C_3^= : C_2^=$		
HZSM-5	(μm)	–	Hydrothermal template synthesis	64	34 – 40	3 – 5	< 70	18, 130
HZSM-5/SAPO-18	–	–	With ZSM-5 nuclei	84	36	1	–	155
P – ZSM-5/SAPO-18	–	–	With ZSM-5 nuclei	83	52	6	–	155
H(Ga)ZSM-5	3 μm	–	Isomorphous substitution of Ga for Al	–	50	8 – 9	> 300	49
H(Fe)ZSM-5	(μm)	–	Isomorphous substitution of Fe for Al	–	38	3 – 4	2	137
H(Al, Fe)ZSM-5	(μm)	–	Isomorphous substitution of Fe for Al	–	49	–	–	141
H(F)ZSM-5	~ 40 μm	High-quality crystals	Template synthesis in fluoride medium	70	45	7.5	> 100	141, 142
H(F)ZSM-5	~ 200 nm	Nanocrystallites	In fluoride medium with silicalite nuclei (nm)	60 – 75	45	5 – 8	305	142
HZSM-5	~ 200 nm	Nanocrystallites	In alkaline medium with silicalite nuclei (nm)	60 – 75	45	5 – 8	157	142
HZSM-5	41 nm	Nanocrystallites	Hydrothermal template synthesis	60 – 70	48	4 – 5	340	156
H(B)ZSM-5	38 nm	Nanocrystallites	Hydrothermal template synthesis	–	48	3.5	1300	144, 156
H(Fe)ZSM-5	50 – 100 nm	Nanocrystallites	Hydrothermal template synthesis	–	34 – 36	17 – 30	–	138, 145
HZSM-5	–	Aggregates [b]	Two-template glucose-assisted synthesis	64	45	8.4	20	146, 147
HZSM-5	20 – 30 nm	Aggregates [b]	With silicalite-1 nuclei (nm) upon adding CTAB [c]	60 – 65	38 – 40	6 – 7	190	148 – 151
H(Si)ZSM-5	–	Aggregates [b]	With tetraethyl orthosilicate	90	44	15	150	105
HZSM-5	72 nm	Nanosheets [b]	Special surfactants were used	80 – 82	45 – 51	5 – 7	103	152 – 154
HZSM-5	10 – 20 nm	Nanosheets [b]	With ZSM-5 nuclei (nm) + surfactant	84	54	7 – 8	168	154
H(B)ZSM-5	10 – 20 nm	Nanosheets [b]	With ZSM-5 nuclei (nm) + surfactant	78 – 80	45 – 50	5 – 6	302	154
			In the presence of H_3BO_3					
H(Mn)ZSM-5	72 nm	Nanosheets [b]	In the presence of surfactant	87	53	4	~ 100	153
H(Ce)ZSM-5	72 nm	Nanosheets [b]	In the presence of surfactant	88	55	5	~ 100	153
H(W)ZSM-5	72 nm	Nanosheets [b]	In the presence of surfactant	82 – 84	54 – 56	5 – 6	> 100	153
ZSM-5/SiC (nanowhiskers)/ SiC (foam)	–	Nanocomposite Whiskers [b]	With SiC nuclei (nanowhiskers)/SiC (foam)	85	51	5 – 6	260	157

[a] Olefin synthesis conditions: 450 – 500 °C, 0.1 MPa, methanol : water = 1 (mol), catalyst mass load with respect to methanol: 1 – 4 h^{-1}; methanol conversion: 99% – 100%.

[b] Hierarchical porous structure.

[c] CTAB is cetyltrimethylammonium bromide.

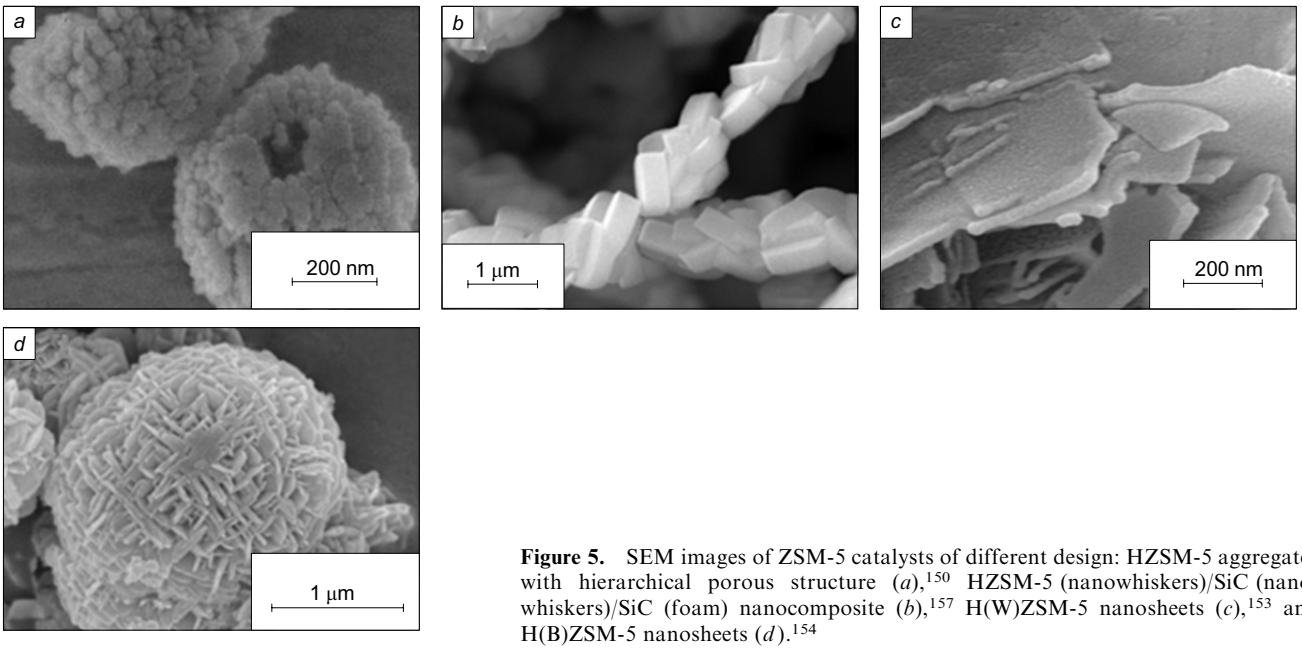


Figure 5. SEM images of ZSM-5 catalysts of different design: HZSM-5 aggregates with hierarchical porous structure (*a*),[150] HZSM-5 (nanowhiskers)/SiC (nanowhiskers)/SiC (foam) nanocomposite (*b*),[157] H(W)ZSM-5 nanosheets (*c*),[153] and H(B)ZSM-5 nanosheets (*d*).[154]

starting mixture leads to a considerable increase in the product yield and in the crystal growth rate; increasing water content leads to formation of larger crystals (221 nm).

Van Grieken and co-workers[159] reported a hydrothermal synthesis of ZSM-5 nanocrystallites. Two types of ZSM-5 aggregates 100 – 200 nm and 400 – 600 nm in size composed of zeolite particles of size 15 – 60 nm and 20 nm, respectively, were obtained at 165 °C from transparent solutions containing sodium ions.[163, 164]

Recently, researchers succeeded in the preparation of nanocrystalline materials with hierarchical porous structure built of spherical aggregates comprised of nanocrystallites linked by meso(macro)pores. To form a hierarchical structure, ZSM-5 nanocrystallites are synthesized using several templates, *viz*., organic amines (they form the microstructure of the zeolite crystal lattice) and mesopore-generating templates (mesoporogens) including cationic surfactants,[152 – 154] organo silanes,[105] carbohydrates,[146, 147, 165] *etc*. Mesoporogens are responsible for the formation of supramolecular mesoporous system that is used for mass transfer of reactants and reaction products.

Inagaki and co-workers[166] proposed a template-free hydrothermal synthesis of ZSM-5 nanocrystallites with hierarchical porous structure in an alkali medium. The absence of expensive organic template reduces the production cost of the nanosized zeolite so it becomes comparable with that of industrial microcystalline zeolite samples.

Yet another recent approach aimed at making the syntheses of ZSM-5 nanocrystallites more economically efficient is to use cheap raw materials.[167 – 173] Attempts have been made to utilize natural materials and aluminosilicate minerals such as rice husk ash,[168] kaolin,[169] rectorite,[170] perlite,[171] diatomite[172] and attapulgite[173] as precursors of silica and alumina for the synthesis of ZSM-5 zeolite. Although these materials are more readily available and cheaper than chemical reagents, direct crystallization of zeolite from aluminosilicate minerals is difficult and still requires auxiliary inorganic substances (*e.g*., liquid glass, silica sol, aluminium hydroxide) or organic templates. The mechanism of such syntheses is still to be clarified, while the results obtained were summarized in a review.[167]

Recently, a novel method for the synthesis of nanocrystallites using ZSM-5 nuclei has been developed.[174 – 178] Nuclei induce crystallization of zeolite and confine the crystal size of the end product. Examples are available of efficient synthesis of ZSM-5 nanocrystallites with hierarchical porous structure using silicalite-1 nuclei in the presence of cetyltrimethylammonium bromide.[148 – 151, 175, 176] Shang and co-workers[154] synthesized ZSM-5 zeolite nanosheets using ZSM-5 seeds in the presence of surfactants.

The available methods for the synthesis of zeolite nanocrystals in an inert matrix (hard template) involve the following stages: mixing of components for zeolite synthesis, addition of hard template, crystallization of zeolite precursors in the presence of the hard template and removal of the template by calcination or dissolution in acids. The templates allow one to control the size of meso(macro)pores and their distribution in the course of synthesis of zeolite materials. The first example of such a synthesis of nanosized ZSM-5 crystals was reported by Jacobsen and co-workers,[179] who used carbon black with pore diameters 31.6 and 45.6 nm as the inert matrix. The size of the zeolite crystals obtained was in the range of 30 – 45 nm, being determined by the pore size of the matrix.

Confined space synthesis with a carbon black matrix was also used[180] to prepare ZSM-5 zeolite nanocrystals with hierarchical porous structure, a specific volume of micro- and mesopores of 0.09 and 1.01 $cm^3\ g^{-1}$, respectively, and mesopore radii in the range of 5 – 50 nm.

Koo and co-workers[181] synthesized ZSM-5 nanocrystals with hierarchical porous structure by microwave treatment of a mixture of precursors of a zeolite gel and carbon black nanoparticles. The zeolite thus obtained was characterized by more developed mesoporosity that the zeolite sample synthesized by the hydrothermal method,.

Carbon nanotubes with inner diameter from 20 to 30 nm (see Ref. 182) and polymers[165, 183] are also used as tem-

plates. When using the hydrothermal method, the main drawback of polymers is that the zeolite crystallization temperature is limited by the thermal behaviour of the polymer, *viz.*, by the glass transition temperature. Polystyrene spheres are most often used. This technique was employed by Xu and co-workers[183] to prepare a zeolite with macroporous structure (pore size from 0.3 to 0.5 nm) formed by ZSM-5 nanocrystals and amorphous aluminosilicate phase. One more kind of a template is starch.[165] It is added into synthetic gel during the synthesis of zeolite and removed when the synthesis is complete by calcination in air. Following this procedure, Liu and co-workers[165] prepared a nanosized ZSM-5 zeolite with lower crystallinity compared to conventional ZSM-5 and higher porosity due to formation of mesopores.

Recently, mixed-topology ZSM-5/SAPO-18 molecular sieves were synthesized using ZSM-5 seeds.[155] High selectivity of these systems to lower olefins (83 – 84%) in the MTO reaction is due to the presence of the SAPO-18 component,[155] while high propylene selectivity (52%) is ensured by promoting the zeolite with phosphorus.

In hetero-substituted MFI-type zeolites,[49, 144, 145, 153] aluminium lattice sites are partially occupied by atoms of other elements (B, Ga, Fe, Mn, W, Ce). When used in the MTO reaction, hetero-substituted systems containing manganese, tungsten and cerium exhibit the highest selectivity to lower olefins (83% – 88%) at a propylene selectivity of 53% – 56% and 100% conversion of methanol.[153] Gallium-substituted zeolite and borosilicate demonstrate a very high stability (catalyst lifetime is longer than 300 h).[49, 144, 154, 156]

The synthesis of ZSM-5 zeolites in fluoride medium[141 – 143] significantly improves the catalyst stability under conditions of the MTP reaction compared to the conventional technique (in alkali medium). Various methods for the preparation of ZSM-5 zeolite nanocrystals with hierarchical porous structure were reported.[146 – 154] In other words, catalytic systems free from internal diffusion constraints and having long catalyst lifetime (> 300 h) under the MTP reaction conditions are now available. High-performance ZSM-5/SiC nanocomposite catalysts (selectivity to lower olefins was 85% at a propylene selectivity of 51%; the lifetime was at least 260 h) were synthesized[157] using zeolite seeds and SiC nanowire layer covered on the SiC foam. However, the best catalytic properties were demonstrated by recently synthesized nanosized borosilicates[144, 154] that retained high catalytic performance even after 1300 h of operation (this is an absolute record among all catalysts of the MTP reaction known so far).

The catalyst selectivity to lower olefins in the DTO reaction can be increased to 97% provided that iron-modified nanocrystalline HZSM-5 zeolites are used and the synthesis is carried out under optimum conditions (temperature is 443 °C, substrate weight hourly space velocity is 18.4 h^{-1}, and hydrocarbon raw material is diluted with inert gas to a DME concentration of 75%).[184]

A study[185] of HZSM-5 zeolite nanocrystals with shortened channels of different length (from 250 to 1 nm) showed that at short contact times, the DTO reaction (DME concentration was 50%) on these catalysts at 350 – 450 °C proceeds with dominant formation of propylene and heavier $C_4^= - C_7^=$ olefins and almost no ethylene is formed. However, DME is not managed to react completely inside very short zeolite channels at high substrate weight hourly space velocities; as a consequence, the conversion is only 60%.

4.4. Post-synthetic treatment of ZSM-5 to prepare nanosized zeolites

Nanosized zeolite materials are mainly synthesized using the bottom-up strategy where the nanostructure is formed by crystallization or targeted aggregation of individual zeolite crystals. There are environmentally and economically costly methods.

An alternative is provided by the top-down strategy which implies selective extraction (removal) of particular components from the synthesized microporous zeolite framework. Methods proposed according to this approach are much simpler and allow one to prepare high-performance catalysts of the MTP reaction based on industrial zeolites.[139, 145] A widely used technique for obtaining nanosized zeolites with developed mesoporosity is to remove, *e.g.*, Al and Si atoms from the zeolite framework.

Dealumination is a well-known post-synthetic procedure for removal of Al atoms from the zeolite structure using chemical agents or hydrothermal treatment. Acid leaching and steaming at high temperatures are most widely used methods for dealumination.[186, 187] In all cases removal of Al atoms is accompanied by partial breakdown of zeolite structure and formation of voids. These voids give rise to additional meso- and microporosity. However, the process is difficult to control, mesopores appear randomly and are poorly interconnected.[188] Besides, removal of framework Al atoms can lead to changes in the acidic properties of the zeolite.[189] For instance, dealumination by steam can cause the appearance of additional out-of-cage acidic Lewis sites.[190] This is beneficial in certain catalytic reactions, but in the case of MTP reaction acidic Lewis sites favour coke formation and accelerate deactivation of the catalyst.[191]

Desilication, one more method for post-synthesis treatment of ZSM-5 zeolites, involves removal of framework silicon under the action of alkali (not only silicon, but also aluminium can dissolve in alkali, although to a much lesser extent). The formation of additional porosity using this technique is accompanied by changes in the structural and acidic properties of the materials, which in turn influences the activity, selectivity and lifetime of the zeolite catalysts.[139, 145, 192 – 194] It was shown[194] that alkali treatment of a zeolite allows one to retain its crystal structure and leads to significant increase in the specific mesopore volume (from 0.072 to 0.279 $cm^3\ g^{-1}$) and a simultaneous decrease in the specific micropore volume (from 0.177 to 0.133 $cm^3\ g^{-1}$). The optimum concentration of NaOH to obtain a developed mesoporosity (> 0.150 $cm^3\ g^{-1}$) without the loss of crystallinity is 0.2 mol L^{-1}; at higher NaOH concentration (1 mol L^{-1}), one deals with amorphization of ZSM-5. Low concentrations of NaOH (0.05 mol L^{-1}) induce the formation of supermicropores about 1.8 nm in size instead of mesopores.[195]

Groen *et al.*[196] considered the effect of the silica modulus in the initial ZSM-5 zeolite on the desilication process. It was established that at low Si : Al ratios (Si : Al < 25), high content of aluminium precludes removal of framework silicon. At Si : Al = 25 – 50, silicon is extracted in controlled manner and desilication is accompanied by the formation of mesopores 9 – 10 nm in size and a specific pore surface area of about 200 $m^2\ g^{-1}$. At high Si : Al ratios (Si : Al > 50), larger pores are formed while the specific mesopore surface area decreases. Desilication allows one to augment the porous system of zeolites with mesoporosity and to create hierarchical structures; however, this is often followed by

the undesired loss of microporosity because it is micropores that contain active sites of the zeolite catalyst.

Breakdown of the synthesized zeolites is a common drawback of desilication and dealumination. This reduces the total yield of reaction products and leads to formation of additional waste products.

Desilication of HZSM-5 zeolite was recently combined with subsequent treatment with aqueous surfactant solution (usually, cetyltrimethylammonium bromide [139, 197, 198] or alkyltrimethylammonium bromide [199]). The interaction between surfactant and zeolite prevents nanocrystals formed under the action of alkali from being broken down and leads to reorganization of the porous system of the zeolite near surfactant micelles. One deals with recrystallization of HZSM-5 zeolite involving transformation of the initially microporous material to a system with hierarchical porous structure.[139, 197 – 199] As a result, aggregates of HZSM-5 nanocrystallites highly stable under conditions of the MTP reaction are formed (catalyst lifetime prior to regeneration for decoking is longer than 400 h).[139] Unfortunately, the zeolite recrystallization technique is costly because it requires surfactants.

The cheapest post-synthesis method for the preparation of nanosized zeolites is to reduce the zeolite particle size mechanically in a planetary or ball mill.[200] However, the particle size distribution obtained upon such a treatment is very wide and attempts to obtain submicrometre-size crystallites are accompanied by amorphization of a large proportion of the crystalline material. Very small zeolite beads (30 000 nm) were ground in a bead milling apparatus.[201] This technique suppresses amorphization during the treatment of the ZSM-5 zeolite. Ground zeolite was treated with alkali solution to dissolve the amorphous fraction and to obtain nanocrystallites 70 – 300 nm in size.

Researchers at TIPS RAS developed a method for preparation of nanosized ZSM-5 zeolites with different Si : Al ratios in an ultrasonic bath.[74, 202] Unlike the ball milled ZSM-5 nanoparticles, those formed under sonication do not require further recrystallization because they retain crystallinity. It was reported [112, 115, 203] that ultrasonically treated Mg – ZSM-5 zeolite nanoparticles efficiently catalyze the DTO reaction, especially when the process is carried out in a slurry reactor.[115, 203]

5. Lower olefins from methane *via* syngas using the Fischer – Tropsch and OX – ZEO methods

The Fischer – Tropsch method involves a direct conversion of syngas to hydrocarbons; therefore, a two-step processing of methane to lower olefins is possible:

$$\text{methane} \longrightarrow \text{syngas} \longrightarrow \text{lower olefins}$$

This route is shorter compared to the processes proceeding *via* methanol or dimethyl ether. At first glance, it looks more attractive.

The Fischer – Tropsch synthesis of hydrocarbons is a mature technology. A number of plants owned by different companies operate in the Republic of South Africa (Sasol), Malaysia (Shell) and Qatar (Qatar Petroleum, Sasol, Shell).[8] However, only liquid motor fuel (mainly diesel) is industrially produced at present,[204 – 207] while lower olefins are obtained in small amounts as side products.

Conversion of syngas to hydrocarbons by the Fischer – Tropsch mechanism proceeds on heterogeneous catalysts (iron, cobalt, ruthenium, *etc.*) [204 – 207] following the laws of surface polymerization and results in a wide range of products (mainly linear alkanes and 1-alkenes having from one to twenty carbon atoms per molecule).[208] At low temperatures, the distribution of reaction products is shifted towards high-molecular-mass linear waxes, while at higher temperatures, the average molecular mass of products is lower and a larger amount of 1-alkenes is formed, which is of interest for production of lower olefins.

Shanghai Yankuang Energy (China) developed a reactor for high-temperature Fischer – Tropsch synthesis and started a pilot plant with a yearly production capacity of 5000 tonnes of olefins and liquid hydrocarbons.[209] This is the first example of semiscale FTSO process (Fischer – Tropsch synthesis of olefins). Cleaned syngas [$H_2 : CO = 1 : 1$ (mole ratio)] is converted to olefins and hydrocarbon oil on the iron-containing catalyst K – Fe – Cu – Al at 300 – 350 °C under a pressure of 1 MPa.[210] Then olefins are separated to isolate ethylene, propylene and butenes.[8] The catalyst activity is rather high (single-pass conversion of CO is 95% – 96%). However, the reaction affords a complex mixture of products including mainly CO_2, methane, ethylene, ethane, propylene, propane, butylene, butane and light hydrocarbon oil.[8] Lower olefins and methane are primary products of CO hydrogenation

$$n\,CO + 2n\,H_2 \longrightarrow C_2H_{2n} + n\,H_2O \quad (9)$$

$$CO + 3\,H_2 \longrightarrow CH_4 + H_2O \quad (10)$$

Carbon dioxide is formed in the water gas shift reaction

$$CO + H_2O \longrightarrow CO_2 + H_2 \quad (11)$$

while alkanes are produced by consecutive hydrogenation of olefins

$$C_2H_{2n} + H_2 \longrightarrow C_2H_{2n+2} \quad (12)$$

The pilot-scale FTSO process has low selectivity (11% – 13%) and therefore the yield of $C_2^= – C_4^=$ olefins is also low (at most 11% – 13%).[210] In addition, the K – Fe – Cu – Al catalyst rapidly deactivates.

At present, there has been considerable research activity aimed at designing selective and stable catalysts of direct conversion of syngas to lower olefins in China, Republic of Korea, Europe, USA and Japan (at SINOPEC, DICP, Tsinghua University, Dow Benelux, Dow Chemical Company, *etc.*). Most studies involve the development of new modifications of iron-containing catalysts of the FTSO reaction.[211 – 224] These efforts are accompanied by the development of novel methods for selective conversion of syngas to lower olefins on hybrid zeolite-containing catalysts.[225 – 227]

Table 5 lists the characteristics of new modifications of iron-containing catalysts of the FTSO reaction. The activity and selectivity of these catalysts to lower olefins is increased by promoting the catalysts with Na/S,[216, 218] K,[211, 212, 215, 228] Mg,[215] Mn,[213, 214, 229] *etc.* This is done in order to accelerate the formation of the active catalytic phase (iron carbide x-Fe_5C_2),[230, 231] to influence the C – C chain growth (by optimizing the yield of $C_2 – C_4$ hydrocarbons and minimizing the formation of methane), to create conditions for suppression of α-hydrogenation (in order to increase the selectivity to olefins compared to

Table 5. Characteristics of new iron-containing catalysts of Fischer – Tropsch synthesis of olefins (weight hourly space velocity is 3000 – 10 000 h^{-1}).

Catalyst	Reaction conditions			CO conversion (%)	Selectivity (%)			O : P [b]	$C_2^= - C_4^=$ yield (%)	Catalyst lifetime /h	Ref.
	T /°C	P /MPa	H_2 : CO		CO_2	CH_4	olefins $C_2^= - C_4^=$ (see [a])				
Fe – Zn – Na	350	2.0	~3	95	16	22	45 (53)	6.9	43	> 100	211
Fe – Zn – K	350	2.0	~3	94	19	21	40 (42)	–	38	–	211
Fe – Al – Na	350	2.0	~3	97	19	21	36 (44)	–	35	–	211
Fe – Zr – Zn – K	340	1.5	2	96	22	17	32 (41)	–	31	> 200	212
Fe – Zr – K	340	1.5	2	94	19.5	16	31 (38)	–	29	–	212
Fe – Cu – Mn/AC	300	2.1	4	98	20	8	24 (30)	5.4	24	> 100	213
K – Fe – Mn/AC	320	2.0	1	85	48	12	20.5 (39)	4.9	17	–	214
K – Mg – Fe/r-GO	340	2.0	1	64	41	12	38.5 (65)	1.2	25	–	215
Fe – Na – S/α-Al_2O_3 (AC)	340	2.0	1	59	45	10	28 (51)	2.7	16.5	–	215, 216
Fe – Na – S/CNT – CN (nanotubes)	340	1.0	2	77	–	8	(47)	6.1	–	> 185	218
Fe – Mn – K/Al_2O_3@Silicalite	340	2.0	1	34	36	18	21 (33)	2.3	7	–	219
Fe@SiO_2 – GC	350	2.0	1	60	–	~10	(41)	4.2	< 20	–	220
Fe/NMC	340	1.0	1	86	46	11	17 (32)	–	15	> 50	221
Fe (nm)/polyaniline	350	2.0	1	79	44	13	26 (47)	4.7	21	> 100	222
Ag – Fe_3O_4 (microspheres) (pore diameter 1.33 nm)	280	2.0	1	71	46	8	23 (43)	5.7	16	–	223
Fe_3O_4@Fe_5C_2 (10 nm)/Fe foil	300	2.0	2	87	22	9	35 (45)	2.4	30	> 200	224
K – Fe – Cu – Al (standard industrial catalyst)	350	1.0	2	95	31	5	11 (17.5)	3.5	~11	–	210

Note. Notations are as follows: AC stands for activated carbon; GO stands for reduced graphene; GC stands for graphite; NMC stands for nitrogen-rich mesoporous carbon; and CNT – CN stands for nitrogen-containing carbon nanotubes.

[a] The content of olefins is given in parentheses.

[b] O : P = olefins $C_2^= - C_4^=$: paraffins $C_2 - C_4$.

paraffins), and to reduce the rate of the water gas shift reaction (to suppress the formation of CO_2).[218] A detailed analysis of the influence of different promoters on the catalytic properties of iron-containing catalysts and of the nature of iron carbide x-Fe_5C_2 was reported in a review.[230] Mention was made that complex chemical composition of composite catalysts precludes unambiguous characterization of the action of promoters. The most pronounced effect was attained by simultaneously modifying the iron catalyst with alkali metals (K, Na) as electronic promoters and with Zn, Al, Zr as structural promoters.[211,212] Catalysts are prepared by co-deposition of metals[211] or by microwave-assisted hydrothermal method.[212] The selectivity of the Fe–Zn–K and Fe–Zn–Na catalysts to lower olefins can reach the range of 40%–45% at a CO conversion of 94%–95%, and the lifetime of the catalysts is more than 100 h. The ratio of the lower olefins to the C_2–C_4 paraffins in the reaction products is nearly 7 : 1, the CO_2 selectivity is lower than 20%, but the content of methane formed is rather high (>20%), which significantly reduces the efficiency of the FTSO process.

Conversion of syngas on supported iron-containing systems (K–Fe–Mn/activated carbon,[214] K–Mg–Fe/graphene,[215] Fe–Na–S/A_2O_3,[211] Fe–Na–S/activated carbon,[212] *etc.*) and on the core–shell catalysts (Fe–Mn–K/Al_2O_3@silicalite,[219] Fe@SiO_2–graphite[220]) affords smaller amounts of methane. The activities of these catalysts are lower than those of the catalysts containing structural promoters (Fe–Zr–K,[212] Fe–Zr–Zn–K,[212] Fe–Zn–K,[211] Fe–Zn–Na[211]) except the system Fe–Cu–Mn/activated carbon[213] (however, its selectivity to lower olefins is only 24%).

The catalytic properties of supported iron catalysts depend not only on the promoter, but also on the type of the substrate (SiO_2,[229,231] Al_2O_3,[211,216] porous activated carbon,[213,214,217] graphite,[220] reduced graphene[215]) and its geometry,[219,220] on the charatecristics of the porous structure[231,232] and on the chemical properties of surface.[233,234] The substrate should facilitate the formation of iron carbide, to maintain the finely dispersed (most active) state of the carbide, to prevent sintering of the active catalytic phase. In this respect, mesoporous silicate and carbon substrates are the best choice.[231,232] Recently, the properties of supported catalysts have been improved by decorating the surface of the carbon substrates with nitrogen-containing functional groups to give nitrogen-rich mesoporous carbon (NMC)[221] or by immobilizing iron on the surface of nitrogen-containing polymers (polyaniline).[222] The former procedure leads to efficient suppression of the formation of methane,[222] acceleration of desorption of lower olefins, exclusion of their hydrogenation and to an increase in the catalyst lifetime to more than 100 h.[222] The formation of lower olefins on the Fe–NMC[221] and Fe–polyaniline[222] systems proceeds with a rather high selectivity (32%–47%) and does not require any structural promoters. The interaction between the metal and the nitrogen-containing carbon substrate is weak, which favours accelerated formation of iron carbide x-Fe_5C_2; that is why such systems exhibit very high catalytic activity. The Fe–NMC catalyst demonstrates a rather high activity of 0.62 g HC h^{-1} g_{cat}^{-1} even at 260 °C (1 MPa, H_2 : CO = 1 : 1); this is much higher than the activities of all iron catalysts known to date under similar conditions.[221]

The activity and stability of catalysts in the FTSO reaction depend not only on their chemical compositions and structure, but also on the particle size.[235,236] As the particle size decreases, the olefins : paraffins ratio in the reaction products increases, the amount of light hydrocarbon products increases[237] and the content of methane decreases.[218,223,224] Nanosized catalytic systems were found to be the most active, stable and selective towards the formation of olefins.[218,223,224]

Iron nanoparticles are synthesized by different methods (water-in-oil emulsion,[237] hydro- or solvothermal synthesis,[223,224] *etc.*). Usually, stable catalysts with high selectivity to lower olefins are prepared by immobilizing iron nanoparticles on carbon materials, such as nanofibres and carbon nanotubes (CNT)[238,239] including nitrogen-containing nanosized substrates (CNT–CN).[218] Conversion of syngas on such systems is free from diffusion constraints, iron carbide is formed much faster, the distance between iron-containing particles can be rather long (this decelerates their sintering) and the catalyst lifetime significantly increases (see Table 5, the Fe–Na–S/CNT–CN catalyst).[218]

Recently, substrate-free nanostructured iron catalysts have been designed, *e.g.*, silver-promoted nanostructured Fe_3O_4 spheres.[223] The catalyst exhibits high activity even at 280 °C. Silver plays an important role in controlling the pore size and the degree of dispersion of iron. The Fe–0.9 Ag catalyst with the smallest pore size (1.33 nm) demonstrated the highest selectivity to lower olefins (43%) at an olefins : paraffins ratio of about 6. It is believed that pores confine the reaction space, which precludes hydrogenation and transport of long-chain hydrocarbon molecules but facilitates hydrogen abstraction and chain growth through insertion of CH_2 units with the formation of lower olefins.

An interesting result was reported by Sun *et al.*,[224] who prepared a nanosized Fe_3O_4@Fe_5C_2 system (species 10 nm in size) on the surface of thin iron foil using controlled hydrothermal growth and calcination). In such a system the metal foil facilitates efficient dissipation of heat released in the course of exothermic FTSO reaction and the catalyst exhibits a record high stability (lifetime > 200 h). The synthesis of lower olefins on Fe_3O_4@Fe_5C_2 nanoparticles on the surface of iron foil is a fast process proceeding without diffusion constraints with rather high selectivity (45%); the amount of methane formed is small (~ 9%) and the CO_2 selectivity is relatively low (22%).

Thus, recently developed (including modern nanotechnologies) modifications of iron catalysts are vastly superior to the industrial catalyst K–Fe–Cu–Al in selectivity and stability. New catalysts allow one to increase the yield of $C_2^=$–$C_4^=$ lower olefins in the FTSO process by 2 to 4 times.

The potential of iron catalysts is limited by the FTSO reaction mechanism. According to the Anderson–Schulz–Flory law, the selectivity with respect to C_2–C_4 hydrocarbons (including olefins and paraffins) cannot be higher than 58%.[240] Nevertheless, a novel method was developed for the synthesis of lower olefins from syngas, which makes it possible to overcome this limit and to obtain lower olefins with selectivity > 70%.[225–227] The innovative oxide–zeolite (OX–ZEO) method has been the focus of activity in a number of research centres in China (DICP, SINOPEC, Xiamen University, Shaanxi Coal and Technology Institute, *etc.*). Syngas is converted on metal oxide–zeolite hybrid catalysts (Table 6).[225–227,241–250] The activation and primary hydrogenation of CO molecule and the formation of the primary C–C bond proceeds on partially reduced oxide

catalyst, a coupling of C—C units occurs in zeolite pores.[225–227] The approach allows one to control the carbon chain propagation and to suppress hydrogenation of the C=C bond and the formation of methane.[226] Lower olefins can be obtained with selectivity in the range of 70% – 80% at a total selectivity towards C_2 – C_4 hydrocarbons to 94% and a methane selectivity of about 2% to 6%.[225] The reaction conditions are as follows: temperature is 400°C, pressure is 1 – 3 MPa and a H_2 : CO mole ratio is 1 – 2.5. The process proceeds in the steady-state mode and the lifetimes of the OX – ZEO catalyst are longer than 100 – 160 h.[227, 247]

Possible oxide components include manganese oxide,[226] Zr—In_2O_3 (catalyst of hydrogenation of carbon dioxide),[243] as well as medium-activity catalysts of the synthesis of methanol [spinel $ZnCrO_x$,[225, 241, 242, 244] $ZnAl_2O_4$,[245, 246] and Zn—ZrO_2 (Refs 227, 247)]. The most active catalyst of the synthesis of methanol, Cu—Zn—Al, is inappropriate for the OX – ZEO process because the reaction on this catalyst results in methanol as the major product and only trace amounts of olefins are available.[251]

The ZEO component of the hybrid catalyst is chosen taking account of the topology and pore size in the crystal lattice. Systems with shape selectivity towards $C_2^=$ – $C_4^=$ olefins are prepared using narrow-pore CHA-type crystallites (SAPO-34[225, 226] and SSZ-13[247]) or mordenite (MOR-type structure).[244, 245] When using mesoporous ZSM-5 zeolites (MFI-type structure), aromatic hydrocarbons (Zn—ZrO_2 + HZSM-5)[252] or C_2 – C_4 paraffins (Cr—Zn—Al/ZSM-5)[253] are formed under identical conditions.

The composition of the 'olefin' product also to a great extent depends on the topology of zeolite (see Table 6). Reactions on mordenite (MOR)-containing systems result in ethylene as the major product (selectivity varies from 65% to 80%),[245, 246] whereas processes on catalysts containing CHA-type molecular sieves (SAPO-34, SSZ-13) proceed with dominant production of propylene ($C_3^=$: $C_2^=$ = 2.5).[247, 248]

There is a synergistic effect of the OX and ZEO components of the hybrid catalyst; if OX or ZEO is absent, the heterogeneous catalyst is almost inactive.[226, 247] The reaction mechanism is still unclear. Intermediate products detected by different authors using physicochemical and kinetic methods are significantly different. Ketene and surface carbonates are detected on $ZnCrO_x$ + SAPO-34,[225, 226] $ZnCrO_x$ + MOR[244] and MnO + SAPO-34[226] systems.[226] Intermediate formation of ethanol was detected in the reaction on multilayer system Zn/Al_2O_4/MOR/Zn/Al_2O_4/MOR;[245] ethylene can be formed upon dehydration of ethanol. The reaction on zirconium-containing hybrid catalysts Zn—ZrO_2 + SSZ-13,[247] Zn—ZrO_2 + SAPO-34,[227] Zr—In_2O_3 + SAPO-34 (Ref. 243) proceeds *via* intermediate formation of methanol and(or) DME, the conversion of syngas to these intermediates being the rate-limiting stage.[247] To date, it is known with certainty[226] that oxygen vacancies on the surface metal oxide play a key role in the dissociation of CO molecule, but the reaction mechanism differs from that of the Fischer – Tropsch synthesis on iron catalysts.[254] Probably, that is why the efficiency of the catalyst decreases upon replacement of the metal oxide component of the hybrid catalyst by iron carbide (Fe/C + SAPO-34 and Fe/C@Si – SAPO-34 catalysts),[248] *viz.*, the selectivity to lower olefins is almost halved while the formation of undesired methane increases from 2% – 6% to 19%.

The catalytic properties of hybrid catalysts depend on both the ratio of the metals in the OX component and the acidity of zeolite,[247] being to the greatest extent affected by the particle size of the catalyst components.[219, 239] Usually, hybrid systems OX – ZEO are prepared by mechanically mixing individual components;[227, 247] therefore, the higher the degree of dispersion of the components of a catalyst the larger the surface area of the contact between individual components. The activity and selectivity of catalysts considerably increase on going from the micro- to nanoscale.[227, 247] High characteristics were achieved upon mixing 4.8-nm Zn—ZrO_2 nanoparticles with 230-nm SSZ-13 nanocrystals[247] and in the reaction on the Zn—ZrO_2 + SAPO-34 nanosized system.[226] The selectivity of the nanosized catalyst Zn—ZrO_2 + SSZ-13 (Ref. 247) to $C_2^=$ – $C_4^=$ olefins reaches a value of 87% at 10% conversion of CO and 77% at 29% conversion of CO [at 400 °C, 3 MPa, and H_2 : CO = 2 (mole ratio)]. The major product is propylene (selectivity 49%) and the catalyst lifetime is longer than 160 h.

Thus, the innovative OX – ZEO method for production of lower olefins from syngas is intensively developing, being attractive from the standpoint of ethylene and(or) propylene selectivity and rather high catalytic stability.[246]

Studies aimed at scaling up the OX – ZEO process using the $ZnCrO_x$ + SAPO-34 hybrid catalyst have been reported.[254] However, the situation is far from large-scale industrialization, in particular, due to certain drawbacks of the method. Lower olefins are produced with high selectivity; however, owing to low activity of the OX – ZEO catalysts and high conversion of CO to CO_2 (> 40%) the yield of the lower olefins is low (12% – 20%) (see Table 6). These values are only slightly different from those achieved on the industrial FTSO catalyst, and in this respect the OX – ZEO systems still cannot compete with the new modifications of the iron catalysts (see Tables 5 and 6).

A concise economic analysis[255, 256] of different technologies of direct conversion of syngas to olefins showed that their feasibility and environmental performance (in particular, lower energy efficiency, higher CO_2 emission) are inferior to the industrial MTO and MTP processes in spite of attractive potential.[256]

Commercialization of FTSO processes is also hampered by the need for large capital investments and energy expenditure for the production of syngas.[14] This is a common problem of all modern large-scale productions in natural gas chemical industry, where methane is activated *via* reforming (high-temperature energy-intensive process).

6. Ethylene and propylene from methane *via* methyl halides

Methods for conversion of methane to olefins *via* halogen derivatives allow one to exclude the expensive energy-intensive stage of methane reforming to syngas from the production cycle and carry out the process in two stages:

methane ⟶ methyl halide ⟶ lower olefins

Methyl halides (chlorinated or brominated hydrocarbons) are obtained from methane using oxidative halogenation or halogenation reactions

Table 6. Characteristics of OX-ZEO hybrid catalysts of direct syngas conversion to lower olefins.

Catalyst	Reaction conditions			Conversion (%)			Content of olefins (%)				$C_2^= - C_4^=$ yield (%)	Ref.
	T/°C	P/MPa	$H_2:CO$	CO	CO_2	CH_4	$C_2^= - C_4^=$	$C_2^=$	$C_3^=$	$C_4^=$		
$ZnCrO_x$ (spinel) + SAPO-34	400	2.5	2.5	22	41 – 45	2 – 3	71 – 80	23	–	–	14 – 16	225, 241, 242
$Zn-ZrO_2$ + SAPO-34	400	1	2	11	–	6	74	–	–	–	–	227
$Zr-In_2O_3$ + SAPO-34	400	2.0	1	28	40	2 – 3	74	–	–	–	12	243
MnO + SAPO-34	400	–	–	8 – 15	–	–	69 – 80	–	–	–	–	218
$ZnCrO_x$ (spinel) + mordenite	400	2.5	2.5	26	~45	2 – 3	> 75	73	–	–	20 – 21	244
$ZnAl_2O_4$ + mordenite	370	3	1	10	–	–	–	65	–	–	–	245
$ZnAl_2O_4$ + SAPO-34	400	1	2	4.5	45	10	77	–	–	–	3.5	246
$Zn-ZrO_2$ (4.8 nm)/SSZ-13 (230 nm)	400	3.0	2	29	41 – 45	3	77	19	49	9	12	247
Fe/C@Si – SAPO-34	340	1.0	1	24	45	19	40	8	20	12	5 – 6	248
$6\,K/100Fe-6\,Cu-16\,AlO_x$ (standard industrial catalyst)	300	1.0	2	96	31.5	5	19.5	6	8	5.5	13	249, 250

$$n\,CH_4 + n\,HX + \frac{n}{2}O_2 \longrightarrow n\,MeX + n\,H_2O \quad (13)$$

$$CH_4 + X_2 \longrightarrow MeX + HX \quad (14)$$

X = Cl, Br

at moderate temperatures (350 – 500 °C).[257] Such a 'low-temperature' approach to activation of CH_4 molecule is very attractive to researchers.

Catalytic oxidative halogenation of methane involves the interaction with hydrogen halide and oxygen [reaction (13)]. In this case, functionalization of CH_4 molecule occurs at < 480 °C under atmospheric pressure.[254, 257 – 259] The reactive halogen generated in the oxidation of methyl halide by oxygen activates a C—H bond in the methane molecule. Methyl halides thus obtained are converted to lower olefins in the second stage by the reaction

$$n\,MeX \longrightarrow n\,HX + C_2H_4 + C_3H_6 + C_4H_8 \quad (15)$$

X = Cl, Br

on zeolite catalysts [SAPO-34,[260, 261] ZSM-5,[262 – 267] ZSM-35 (Ref. 269), *etc.*].

The two-stage process of production of $C_{\bar{2}} - C_{\bar{4}}$ olefins from methane *via* methyl chloride is proven at the Research and Engineering Centre 'Sintez' (Moscow, Russia).[269 – 272] Oxidative chlorination of methane is carried out at 300 – 400 °C in fluidized-bed reactors. The catalysts are supported copper chloride[269] or a mixture of copper chloride, potassium chloride and lanthanum chloride (in a 1 : 1 : 0.3 mole ratio) supported on a porous substrate.[272] The catalyst lifetime can be as long as 4000 h under optimum conditions. In the second stage methyl chloride is converted to lower olefins in fluidized-bed reactor on SAPO-34-type silicoaluminophosphate catalyst at 425 – 450 °C at pressures in the range of 0.2 – 0.5 MPa.[270, 272] The conversion of methyl chloride reaches 75% – 80%, while ethylene and propylene are formed with a selectivity of 45% and 35%, respectively.[270] The highest selectivity to the sum of ethylene and propylene (up to 87%) is observed at a certain degree of carbonization of the catalyst (2.6 mass % – 5.2 mass %). Hydrogen chloride is returned to the stage of oxidative chlorination of methane. The catalyst is regenerated by air at 550 °C until complete recovery of its activity.

The MCTO was proposed for the synthesis of olefins at chlorine plants. A feasibility assessment[269] revealed higher profitability of the MCTO process compared to the industrial MTO method, *viz.*, the absence of energy-intensive and material-intensive stage of syngas production reduces the capital investments by 25% and the methane consumption decreases by 10%. However, the MCTO product almost always contains organochlorine impurities (CH_2Cl_2, MeCl, CCl_4).[273] The olefins produced are suitable for production of basic chlorine-containing chemicals (dichloroethane, vinyl chloride, polyvinyl chloride),[274] but do not meet the requirements for polymer-grade production as monomers for the synthesis of polyethylene and polypropylene. At present, domestic chemists work hard to solve this problem.[271, 273]

The MCTO method developed in the Russian Federation is aimed at producing lower olefins with dominant formation of ethylene.[259, 270] Researchers from the Xiamen University (China) proposed a two-stage technology of methane conversion to propylene *via* methyl chloride or methyl bromide[275] using original highly efficient new-generation catalysts (CeO_2 nanocrystals, fluorinated zeolite H(F)ZSM-5). Oxidative chlorination of methane is carried out on $FeO_x - CeO_2$ nanorods at 480 °C and atmospheric pressure and affords methyl chloride with a selectivity of 74% at a CH_4 conversion of 23%. Efficient oxidative bromination of methane requires more severe conditions (600 °C) and NiO/CeO_2 nanocubes as catalyst. The selectivity to MeBr is 82%, at a methane conversion of 22%. The catalyst lifetime is longer than 100 h. The second stage of the process, *viz.*, conversion of methyl halides, is carried out on fluorinated zeolite H(F)ZSM-5 at 400 °C. Propylene is obtained in yields of 41% – 49% from MeCl and 53% from MeBr with a selectivity of 46% – 64% and 56%, respectively. The reaction proceeds in a steady-state mode over a period of at least 50 h.

One-pot conversion of methane to lower olefins *via* chlorination without isolation of intermediate product (methyl chloride) proposed at the University of South California (USA)[28] allows one to simplify the flow diagram of the process to one reaction unit. Chlorination of CH_4 [reaction (14)] and conversion of MeCl to hydrocarbons [reaction (15)] are carried out on the same catalyst (SAPO-34) in one reactor at the same temperature (350 °C) and pressure (0.1 MPa). The reactions proceed consecutively and, depending on the contact time and on the time on stream, one can obtain either methyl chloride or olefins. Gaseous halogen highly diluted with methane ($CH_4 : Cl_2 = 10 : 1$) is used as raw material. Chlorination of methane on the surface of SAPO-34 leads to selective formation of methyl chloride. After 2h on-stream (contact time was 60 s) only MeCl is detected in the reaction products at a conversion of chlorine of 92%. After 18 h on-stream, the reaction products contain about 40% of lower olefins (~23% ethylene, ~14% propylene, ~6% butenes). Bromination of methane on SAPO-34 can be performed analogously, but the process is much less efficient. The yield of methyl bromide in the initial stage of the reaction is at most 49%, while the developed process yields propane (~28%) as the major product rather than ethylene (15%) or propylene (7%).

Lower olefins synthesized using the MCTO processes and industrial processes, MTO and MTP, are obtained on the same-type catalysts (SAPO-34,[257, 261] and ZSM-5[262 – 267]). Methyl halides and methanol are structurally similar and the catalytic properties of the zeolite catalysts of the MCTO and MTO reactions depend on the same factors (crystal lattice type, acidity, *etc.*).[257, 268, 275] The effect of the zeolite topology, the silica modulus and different modifiers on the behaviour of the catalyst in the MCTO reaction was considered in a review.[257] New catalysts of the MCTO reaction are designed using modern methods of nanotechnology, thus following the strategy for the design of catalysts of the MTO and MTP processes. This approach allows one to prepare more stable catalysts of the conversion of methyl chloride to lower olefins.

The lifetime of recently synthesized[261] nanosized silicoaluminophosphate SAPO-34 in the MCTO reaction is two times longer than that of the traditional SAPO-34 catalyst. The nanosized SAPO-34 was prepared using an original 'dry' gel procedure involving azeotrope drying and steam-assisted crystallization without using expensive templates or specially synthesized starting materials.

A ZSM-5 zeolite with hierarchical porous structure was synthesized.[263, 264] Conversion of methyl chloride to hydro-

carbons on this catalyst proceeds at 450 °C with an efficiency of more than 98% and the selectivity to lower olefins reaches a value of 68%. The new catalyst, which is 4.5 times more stable than conventional ZSM-5, was prepared by controlled crystal growth under hydrothermal crystallization conditions in the presence of triethoxyvinylsilane used as nanocrystallite growth inhibitor.[263]

A stable catalyst based on ZSM-5 zeolite can also be prepared by coating the external surface of ZSM-5 with a layer of polycrystalline silicalite-1, which passivates the acid sites on the zeolite surface.[262] Lower olefins are formed from methyl bromide on the core–shell HZSM-5@silicalite-1 catalyst at 450 °C with a selectivity of more than 80% at a conversion of MeBr of 75%–80%. The lifetime of this catalyst is longer than 120 h (*cf.* at most 40 h for traditional HZSM-5 catalyst under identical conditions).

7. Oxidative coupling of methane to ethylene

The oxidative coupling of methane has long been attracting the attention of researchers as promising one-step route from methane to ethylene. A new period of intensive studies on this reaction began in 2008 at certain research and commercial centres, *e.g.*, Dow Chemicals, Fina Technology, Siluria Technology, Sabic Global Technologies, King Abdullah University of Science and Technologies (KAUST), Russian Academy of Sciences, Chinese Academy of Sciences, SINOPEC, *etc.* The results obtained were summarized in reviews (see, *e.g.*, Refs 15–18) and more than 30 new publications appear yearly.

The oxidative coupling of methane to ethylene + ethane mixture is carried out in the presence of heterogeneous catalysts based on alkaline-earth metal oxides,[276,277] rare-earth metal oxides,[277–280] tin oxide,[281,282] manganese oxide,[283] *etc.* at 550–1000 °C. Manganese-containing composites Na(K, Li, Rb)–MnW/SiO_2 are active at temperatures above 800 °C and exhibit the highest stability and selectivity to C_2H_4.[284]

The process can be described by the equation

$$2\,CH_4 + O_2 \longrightarrow C_2H_4 + 2\,H_2O \qquad (16)$$

Actually, the reaction proceeds *via* formation of ethane

$$2\,CH_4 + \frac{1}{2}O_2 \longrightarrow C_2H_6 + H_2O \qquad (17)$$

which undergoes oxidative dehydrogenation [18]

$$C_2H_6 + \frac{1}{2}O_2 \longrightarrow C_2H_4 + H_2O \qquad (18)$$

This is a semicatalytic process;[285] at temperatures above 600 °C, the formation of ethane (ethylene) can proceed without a catalyst.[286] The OCM mechanism involves multiple surface catalytic reactions and gas-phase homogeneous reactions,[18,287] the contribution of the latter being increased with increasing temperature. The activation of methane molecule occurs on the surface of the catalyst with the formation of methyl groups that can be desorbed to the gas phase in the form of free radicals ($CH_3^{\bullet}$) at temperatures above 800 °C. In the gas phase, methyl radicals undergo homogeneous recombination to ethane molecules that subsequently undergo dehydrogenation to ethylene. At lower temperatures, the activation of methane and oxygen molecules on the catalyst surface can be accompanied by the formation of ethane and ethylene; these reactions can proceed on different oxygen sites.[288,289] For instance, a recent study [289] revealed that dissociation of O_2 molecule on the $NaMnW/SiO_2$ composite catalyst is followed by the formation of the $Mn^{5+}{=}O$ active site responsible for the methane activation *via* the formation of $Mn^{4+}-O^{\bullet}$ and that recombination of methyl radicals occurs on the oxide site $W^{6+}{=}O$ with the formation of methoxy groups bound to W^{5+}.

The reaction products, ethane and ethylene, are thermodynamically less stable and more reactive than the stable methane molecule.[14] Therefore, conversion of methane to C_2 hydrocarbons is accompanied by their fast oxidation to carbon oxides, which complicates the production of ethylene with high selectivity.

To avoid the oxidation of the C_2 products, the OCM reaction is carried out under oxygen deficiency conditions (at a $CH_4:O_2$ mole ratio of 3–10). This limits the conversion of methane on different heterogeneous catalysts to 20%–45%. The yield of ethylene is at most 16%–18% even if the most selective catalysts are used.[279,290–292] The maximum conversion of methane and the energy efficiency are less than 30%, being two times lower than for production of ethylene by pyrolysis of naphtha.[293] Therefore, today the OCM method is unattractive to industry. To make it cost efficient,[293,294] one should increase the yield of ethylene to 30%–50% (based on different estimates), increase the conversion of methane and(or) reduce the reaction temperature.[293]

The main strategies for solving these problems involve the development of new methods for carrying out the OCM reaction and new reactor designs, as well as the design of selective and stable catalysts with high activity at moderate temperatures. A general trend of R&D activity in this field is to increase the contribution of catalytic reactions to the formation of ethane(ethylene) and to reduce the contribution of the homogeneous gas-phase component in order to increase the controllability of the process.

Modern laboratory-scale methods for the synthesis of C_2 hydrocarbons by the oxidative coupling of methane differ in feed supply modes, temperature and catalysts, type of reaction unit and reactor design (adiabatic, fluidized-bed, membrane, 'chemical looping', *etc.*) (Table 7).[283,288,294–313]

In the innovative approaches to the OCM reaction, such as 'chemical looping' [298–303] and membrane reactors,[304–309] oxygen is fed to the reaction section in distributed mode, which creates prerequisites for selective formation of target products. According to the results of cost efficiency analysis,[293] this enables a 15% increase in the conversion of methane and thus reduces the production cost of ethylene. In the case of 'chemical looping' [298–303] methane and oxygen are fed separately, in alternative manner or to different reactors, the two-reactor unit with the catalyst circulating in the fluidized layer being the most efficient.[300,302,303] One reactor is used for the oxidation of methane in the absence of gaseous O_2 (with lattice oxygen as catalyst). This almost completely excludes gas-phase reactions and undesired oxidation of the C_2 products. 'Deoxygenated' catalyst is transferred to the second reactor and regenerated by atmospheric oxygen.[302,303] Thus, the process occurs within the framework of the redox system with alternate reduction (by methane) and oxidation (by oxygen) of the oxide catalyst. In this process the oxidative regeneration of the catalyst surface can be achieved using not only pure oxygen, but also air. Manganese-containing catalysts $NaMnW/SiO_2$,[298–301] Mg_6MnO_8 (Ref. 302) and $Li-Mg_6MnO_8$ (Ref. 303) are

Table 7. Modern methods of conducting oxidative coupling of methane to ethylene (as mixture with ethane).

Process type, reactor type	CH_4 and O_2 feed mode	Catalyst	T/°C	CH_4 conversion (%)	Selectivity (%)		Single-pass yield (%)		Ref.
					$\sum C_2$	$C_2^=$	$\sum C_2$	$C_2^=$	
High-temperature semicatalytic process in adiabatic reactor or in fluidized-bed reactor	Mixed raw material $CH_4 : O_2 = 3-4$ (see [a]), pressure 0.1 MPa	$NaMnW/SiO_2$	800 – 1000	20 – 37	65 – 83	38 – 44	16 – 32	15 – 162	283, 288, 294 – 296
		$LiMnW/SiO_2$	~900	43	46	35	20	15	297
		$La_2O_3 - CeO_2/SiO_2$	905	28	64	45	18	13	279
'Chemical looping', two-step redox system (fluidized-bed reactors), OCM in the absence of oxygen in the gas phase (with lattice oxygen as oxidizing agent)	Cyclic, periodic or alternating supply of CH_4 and O_2 to two different reactors), alternating oxidation – reduction of catalyst	$NaMnW/SiO_2$	750	–	–	–	23 – 25	–	298 – 301
		Mg_6MnO_8	840	23 – 38	66 – 83	27 – 35	23	13	302, 303
In membrane reactor	Continuous supply of CH_4, distributed oxygen supply *via* an O^{2-}-permeable membrane	$NaMnW/SiO_2$/ceramic membrane	825 – 850	26.5 – 37	65 – 72	52	19 – 24	14	295, 304
		$NaMnW/SiO_2$/BSCF [b]	900	–	70	–	3 – 16	–	305
		$NaMnW/SiO_2$/MIECM [c]	850	52	68	40	35	21	306
		BYS/nano-LSCF,[d]	900	49	79	–	39	–	307
		BCG hollow fibre [e]	750	14	71	32	10	5	308
'Low-temperature' thermocatalytic process	Mixed raw material $CH_4 : O_2 = 4$ (see [a]), pressure 0.9 MPa	La_2O_3, nanowire	550 – 560	25 – 27	50 – 54	–	14	–	309, 310
	Mixed raw material, pressure 0.1 MPa	$Sr - La_2O_3$, nanofibre	500 – 650	35 – 38	47 – 52	25 – 35	15.5 – 20	9 – 14	311
Microwave-assisted process	Mixed raw material $CH_4 : O_2 = 4$ (see [a])	$Na_{10}Mn_2W_5/SiO_2 + WC$	750	27	64	–	17	–	312
In low-temperature plasma corona discharge	Mixed raw material $CH_4 : O_2 = 4$ (see [a])	Zeolite HY (no zeolite)	25	85 (55)	70 (58)	–	59 (32)	–	313

[a] Volume ratio.
[b] BSCF stands for $Ba_{0.5}Sr_{0.5}Co_{0.8}Fe_{0.2}O_{3-\delta}$.
[c] MIECM stands for mixed ionic-electronic conducting membrane.
[d] BYS stands for $Bi_{1.5}Y_{0.3}Sm_{0.2}O_{3-\delta}$; LSCF stands for $La_{0.6}Sr_{0.4}Co_{0.2}Fe_{0.8}O_{3-\delta}$.
[e] BCG stands for $BaCe_{0.8}Gd_{0.2}O_{3-\delta}$.

used as both catalysts and the source of lattice oxygen. These systems exhibit high oxygen capacity, *e.g.*, nearly 20 mmol g_{cat}^{-1} for the $NaMnW/SiO_2$ composite.[298] Oxidative coupling of methane in the 'chemical looping' mode at 840 °C is characterized by high ethane and ethylene selectivity of 45%–50% and 27%–35%, respectively.[302] The operating characteristics of the catalyst do not deteriorate after more than 100 cycles and its lifetime is at least 50 h. But the yield of C_2 hydrocarbons almost never exceeds 25%.[298–303] It is believed[300] that hydrogen formed in the dehydrogenation of ethane competes with methane for the active sites, and this competition limits the rate of the target reaction. Therefore, progress of the 'chemical looping' method is associated with an increase in the pressure of methane or with reduction of the reaction temperature to less than 750 °C for partial suppression of the dehydrogenation of ethane.[300]

Yet another innovative approach to the OCM reaction is to use membrane reactors.[304–309] Similarly to the 'chemical looping' method, this one also provides a high selectivity of formation of C_2 products and allows one to use atmospheric air instead of pure oxygen. The operating principle, design and various configurations (fixed-bed, ionic-electronic, disc-shaped, tubular, *etc.*) of membrane reactors have been considered in detail in a review[16] and in original publications.[295, 304–309] In the membrane reactors, oxygen is supplied to the reaction section through the surface of a capillary O^{2-}-permeable membrane in the distributed mode. Usually, the design of membrane reactors includes a combination of a selective catalyst, mainly O^{2-}-conductive type ($NaMnW/SiO_2$, perovskites), with O^{2-}-permeable ceramic membrane based on perovskites.[295, 304, 305] Bhatia *et al.*[306] developed a mixed ionic-electronic oxygen-permeable membrane coated with a layer of the Na–Mn–W catalyst. This catalytic membrane reactor was used to obtain C_2 hydrocarbons from methane at 850 °C in 35% yield with an ethylene selectivity of 40%.[306] Othman *et al.*[307] developed a membrane reactor using a $La_{0.6}Sr_{0.4}Co_{0.2}Fe_{0.8}O_{3-\delta}$ hollow fibre coated with a thin (300–500 nm) layer of $Bi_{1.5}Y_{0.3}Sm_{0.2}O_{3-\delta}$ catalyst deposited by the sol–gel method. They obtained a record high yield of C_2 products in the OCM reaction, *viz.*, 39% at nearly 50% conversion of methane and a C_{2+} selectivity of 79%. The efficiency of this membrane system is due to uniform dispersion of catalyst nanoparticles that provide higher oxygen permeation rate through the membrane. The membrane reactors described above efficiently operate at high temperatures (850–900 °C).[304–309] Recently, researchers at ExxonMobil[308] synthesized a membrane catalyst of the composition $BaCe_{0.8}Gd_{0.2}O_{3-\delta}$, which reduced the temperature of the OCM reaction to 750 °C.[308] This offers new prospects for the development of the 'membrane' approach at moderate temperatures.

Carrying out the OCM reaction using membrane reactors or 'chemical looping' reaction units offers the following advantages over traditional procedure using mixed raw material ($CH_4 + O_2$):

— complete exclusion of capital investment and energy expenditure for maintenance of the installation for cryogenic separation of atmospheric oxygen,

— the absence of direct contact between gaseous oxygen and methane, and

— the absence of reactions outside the catalytic layer.

Innovative methods with distributed supply of methane and oxygen offer a great economic potential owing to considerable reduction of energy expenditure and CO_2 emission;[293, 302] however, they are rather complicated. Therefore, there has been research activity aimed at improving technologically simpler thermocatalytic OCM processes with continuous supply of mixed raw material.

On the one hand, researchers continue to develop high-temperature process using the most selective composite catalyst $NaMnW/SiO_2$,[294–297] in particular, they optimize its chemical compositions,[290, 291, 314, 315] study the kinetics and mechanism of the reaction[288, 289, 316–318] and consider different types of reactors (microchannel, staged, fluidized-bed, *etc.*).[319] On the other hand, innovative 'low-temperature' versions of the OCM process[310, 311] using high-performance nanostructured catalysts based on rare-earth element oxides operating at temperatures below 650 °C are under development. A cost efficiency analysis[293] showed that, economically, the reduction of temperature below 650 °C is no less efficient than the use of membrane reactors and the 'chemical looping' concept. The 'low-temperature' approach allows one to reduce the production cost of ethylene by 15%. Non-traditional methods were also proposed to carry out the OCM reaction (Table 7).[312, 313] For instance, microwave-assisted activation of methane on the $NaMnW/SiO_2$ catalyst supported on tungsten carbide allowed the temperature of the OCM reaction to be reduced to 750 °C.[312] An original method for carrying out the OCM reaction in corona discharge of low-temperature plasma on the surface of HY zeolite at room temperature and atmospheric pressure was reported.[313] A very high conversion of methane to C_2 hydrocarbons and a record high yield of C_2 products equal to 59% were achieved at a $CH_4 : O_2$ mole ratio of 4 and a gas flow rate of 4 mL min^{-1}. However, this technique is hardly suitable for large-scale production of ethylene(ethane).

Siluria Technology (USA) attempted to industrialize the OCM process.[320] The company patented the 'low-temperature' design which combines the oxidative coupling of methane at 540–650 °C with oxidative dehydrogenation of ethane at 650–830 °C.[310, 321–324] The process is based on the use of La_2O_3, Li/MgO, *etc.* nanowire catalysts.[310, 321–324] In 2014, Siluria and Braskem America started a pilot plant with a yearly production capacity of about 400 thousand tonnes of ethylene.[320] It was assumed to integrate the process with a natural gas liquefaction system or with a system for pyrolysis of ethane.[322] However, most innovations claimed by Siluria including information on non-traditional microbial synthesis of 'nanowire' catalysts and their efficiency were not confirmed.

Researchers at various scientific centres develop new 'low-temperature' nanosized catalysts of the OCM reaction with different morphology[325–331] (Table 8). Nanowire catalysts based on manganese and titanium oxides were synthesized.[325] A series of catalytic systems based on rare-earth element (Sm, Tb, Ce, Pr) oxides supported on magnesium oxide nanoparticles was prepared.[326] A wide range of nanostructured catalysts Sm_2O_3 (Ref. 327) and La_2O_3 (Refs 311, 330) with different design (nanobelts, nanorods, nanotubes, nanosheets, nanoflowers, nanofibres) is available.[311] Recently, $La_2O_3-CeO_2$ nanofibre catalysts have been obtained.[287, 331] Different authors demonstrated that the catalytic properties of nanosized catalysts depend on their chemical composition[310, 327] and design.[328, 329] For instance, La_2O_3 nanoparticles exhibit low efficiency at 500–550 °C, whereas nanostructured systems with more developed external surface used in the OCM reaction carried out in the

Table 8. Characteristics of nanosized catalysts for oxidative coupling of methane (pressure of 0.1 MPa, at O_2 conversion of ~100%).

Catalyst	T/°C	$CH_4:O_2$	CH_4 conversion (%)	Selectivity (%)		Single-pass yield (%)		Ref.
				$\sum C_2$	$C_2^=$	$\sum C_2$	$C_2^=$	
Mn/TiO_2, nanowire	750 – 775	5	14 – 16	35 – 50	14 – 25	4.5 – 7.5	2 – 4	325
Sm_2O_3/MgO, nanoparticles	650 – 700	4	21 – 22	50 – 52	26	11	6	326
$Li-Sm_2O_3$/MgO, nanoparticles	650 – 700	4	21 – 24	63 – 64	38	13 – 15	8	326
TbO_x/MgO, nanoparticles	650 – 700	4	17 – 18	39 – 41	16	7	3	326
$Li-TbO_x$/MgO, nanoparticles	650 – 700	4	23	64	37	15	9	326
CeO_2/MgO, nanoparticles	650 – 700	4	14	12 – 15	7	2	1	326
$Na-CeO_2$/MgO, nanoparticles	650 – 700	4	22 – 23	56 – 57	27	12 – 13	6	326
PrO_y/MgO, nanoparticles	650 – 700	4	16 – 17	32 – 36	14	5 – 6	2	326
$Li-PrO_y$/MgO, nanoparticles	650 – 700	4	16 – 21	58 – 61	39	9 – 13	8	326
$Na-PrO_y$/MgO, nanoparticles	650 – 700	4	19 – 20	47 – 48	19	8.5 – 9.5	4	326
Sm_2O_3, nanobelts	500 – 600	3	27 – 28	40 – 42	–	11 – 12	–	327
Sm_2O_3, nanorods	500 – 600	3	26 – 27	37 – 38	–	10	–	327
Sm_2O_3, nanotubes	500 – 600	3	25 – 26	33 – 34	–	8 – 9	–	327
$Sr-Sm_2O_3$, nanobelts	600	3	29	48	–	14	–	327
$Sr-Sm_2O_3$, nanorods	600	3	29	48	–	14	–	327
$Sr-Sm_2O_3$, nanotubes	600	3	28	47	–	13	–	327
La_2O_3, nanowires	550 – 650	4 [a]	25 – 27	50 – 54	–	14	–	310
La_2O_3, nanoparticles	500	3	2	0	–	0	–	328, 329
La_2O_3, nanoparticles	550	3	10	6	–	6	–	328
La_2O_3, nanorods	500 – 550	3	29	41 – 45	–	12 – 13	–	328 – 330
La_2O_3, nanosheets	500 – 550	3	31 – 32	37 – 46	–	11 – 15	–	328
La_2O_3, nanoflowers	500 – 550	3	27 – 29	35 – 42	–	9 – 12	–	328
$La_2O_3-CeO_2$, nanofibres	470 – 520	7	28 – 29	65 – 70	–	18 – 20	–	331
$La_2O_3-CeO_2$, nanoparticles	540 – 630	7	8 – 13	60 – 70	–	5 – 9	–	331
$La_2O_3-CeO_2$, nanofibres	570	7	23	64	24	15	6	287
$La_2O_3-CeO_2$, nanofibres	610	9	18	70	25	13	5	287
$Sr-La_2O_3$, nanofibres	500 – 650	–	35 – 38	47 – 52	25 – 35	15.5 – 20	9 – 13	310

[a] At a pressure of 0.9 MPa and a feed space velocity of 130 000 h^{-1}.

same temperature range are characterized by a conversion of methane of nearly 30% and a selectivity in the range of 35% – 46%; the yield of C_2 hydrocarbons reaches 9% to 15%;[328, 329] the highest efficiency was reported for 2D nanostructures (nanobelts,[327] nanosheets [328]). A series of independent studies [287, 326, 327, 331] showed that the selectivity of the catalysts based on the rare-earth element oxides can be increased to 52% – 70% by doping them with ceria [287, 331] or with alkali (alkaline-earth) metals [326, 327] (in the latter case, the catalysts become more stable). The $Sr-La_2O_3$ nanofibrous catalyst [311] exhibits the highest efficiency. Namely, it provides nearly the same yield of ethylene (up to 13%) at 500 – 650 °C as that reported for the most selective high-temperature catalyst $NaMnW/SiO_2$ operating at ~900 °C.[284] The lifetime of the $Sr-La_2O_3$ nanofibres is about 100 h.

Sucessful development of nanostructured catalysts is accompanied by studies on the possibility to reduce the temperature of the synthesis of C_2 hydrocarbons on $NaMnW/SiO_2$-type catalysts and on other traditional systems.[332] The results obtained in 2018 are collected in Table 9. A number of novel catalysts active at temperatures below 750 °C were designed, including new modifications of manganese-containing composites,[332 – 335] systems based on iron oxide,[336] tin oxide,[281, 282] and rare-earth element oxides.[277, 280, 296, 337] Most new catalysts allow the temperature of the OCM reaction to be reduced to 700 – 750 °C (see Table 9). Catalytic systems active at about 650 °C are available.[277, 280, 337] They are based on Sr-promoted lanthanum oxide ($Sr-La_2O_3$/cordierite,[280] $Sr-La_2O_3$/MgO,[277] $Cs-Sr-La_2O_3$ [296]). A microscale system $Cs-Sr-La_2O_3$ prepared [296] by promoting lanthanum oxide with strontium and caesium approaches nanostructured catalysts in efficiency. The system kicks into gear at 500 °C and provides a conversion of methane of ~25%, although being somewhat

Table 9. Characteristics of catalysts for oxidative coupling of methane at temperatures $\leqslant$750 °C (see [a]).

Catalyst	T/°C	$CH_4:O_2$	CH_4 conversion (%)	Selectivity (%)		Single-pass yield (%)		Ref.
				$\sum C_2$	$C_2^=$	$\sum C_2$	$C_2^=$	
$Na_7Mn_{17}W_{1.5}/Si_{100}O_x$ (for comparison)	800	3	42 – 43	56	38	24	16	290
$Na_{10}Mn_2W_5/SiO_2$	750	3	11	69	36	8	4	332
$Na_{12}Mn_{14}Mo_{15}/SiO_2$	750	3	40	47	33.5	19	13	332
$Na_2WO_4 - Mn/(MgO - TiO_2)$	775	2	–	–	–	16.5	14	333
$TiO_2 - NaMnW/SiO_2$ ($MnTiO_3$)	700	4 – 5	23 – 24	73 – 74	–	17	–	334
$Ag - Mn - Na_2WO_4/SiO_2$	725	4	18	78	33	14	6	335
$Ag - Mn - Na_2WO_4/SiO_2$ + $Ce - Mn - Na_2WO_4/SiO_2$	750	4	20	78	–	16	–	335
$HF - Fe_2O_3$ (ferrospheres)	750	8	4	73	25	3	1	336
Li/SnO_2	750	4	13	~70	–	9	–	282
Li/SnO_2 + LiC	750	2.5	34	55	47	18.5	16	281
$CeO_2 - Y_2O_3$	750	4	22	47	–	10	–	337
$La_2O_3 - CeO_2$ + $Ce - Mn - Na_2WO_4/SiO_2$	700	4	31	71	40	22	12	335
$Sr - La_2O_3$/cordierite	650 – 700	8	21 – 22	68 – 72	–	14 – 15	–	280
$Cs - Sr - La_2O_3$	500 – 550	3	25	38	–	10 – 14	–	296

[a] Reaction conditions: a total pressure of 0.1 MPa and a feed space velocity of 7200 – 20 000 h^{-1}, and O_2 conversion of about 100%.

inferior to nanosystems in the selectivity towards C_2 hydrocarbons (38%) and stability (lifetime to 50 h).

Thus, at present systems based on lanthanum oxide promoted with alkali and alkaline-earth metals (see Tables 8 and 9) are the most efficient microscale and nanosized catalysts of the OCM reaction at temperatures of at most 650 °C.[280, 296, 310] The active sites of the OCM reaction and the mechanism of the action of promoters have been thoroughly reviewed.[15, 18] Most researchers hold the view that the mechanism of the reaction on the rare-earth element oxides, at least at 550 – 650 °C, differs from the redox mechanism characteristic of other catalysts. It is believed [15, 294, 338] that the activation of methane on lanthanum oxide to a greater extent proceeds by the ionic mechanism on the acid-base sites of the $La^{3+} - O^{2-}$ pair *via* the formation of the intermediate $CH^{3-} - La^{3+} - OH^-$ with CH_4 being treated as a very weak acid.[338] The strength of the basic sites (O^{2-}) can be influenced using promoters (alkali or alkaline-earth metals like Sr, Cs, *etc.*), which provides new opportunities for controlling the OCM reaction.

One can say that at present, a new line of research, carrying out the OCM reaction on rare-earth element oxides at temperatures below 650 °C has actually formed.

Room-temperature activation of methane by oxygen on Zn – ZSM-5 zeolite was reported.[339] Using solid-state NMR and other physicochemical methods and DFT† calculations, it was shown that methane activation proceeds in dual manner by homolytic cleavage of the C – H bond on the oxygen-containing zinc clusters with subsequent formation of methyl radicals and by heterolytic dissociation on Zn^{2+} ions in the zeolite framework *via* the formation of the surface methoxy groups. The latter mediate the formation of methanol and its further conversion to hydrocarbons. Therefore, one cannot rule out that a new 'low-temperature' approach to the OCM reaction, *viz.*, carrying out the process on the surface of metal oxide-promoted zeolites will be proposed in the nearest future.

At present, modified zeolite-containing catalysts are used in the non-oxidative coupling of methane.[30, 31]

8. Non-oxidative coupling of methane to ethylene

Similarly to the OCM reaction, non-oxidative coupling of methane allows one to convert methane to ethylene(ethane) in one step

$$2\,CH_4 \rightleftharpoons C_2H_4 + 2\,H_2 \quad (19)$$

$$2\,CH_4 \rightleftharpoons C_2H_6 + H_2 \quad (20)$$

This method of direct conversion of methane to C_2 hydrocarbons excludes the non-productive conversion of methane to carbon oxides (main drawback of the OCM process). However, thermodynamic constraints on the Non-OCM reaction are more severe and the process requires higher temperatures than the OCM reaction.[16] In addition, it is difficult to arrest the reaction in the 'ethylene(ethane)' stage. Ethylene undergoes rapid condensation into aromatic hydrocarbons and coke species.[11, 16] The Non-OCM process can hardly be used to obtain the C_2 products with high selectivity; usually, it is utilized for the synthesis of aromatic hydrocarbons mainly on molybdenum carbide supported on zeolites.[11, 340]

† Density Functional Theory.

Methane was converted to ethylene with high selectivity (> 90%) by the Non-OCM reaction on molybdenum carbide supported on boron-substituted ZSM-5 zeolite (Mo_2C/[B]ZSM-5) at 700 °C and atmospheric pressure.[30] Owing to low acidity of the zeolite substrate the oligomerization of ethylene was suppressed, no coke formation was observed and the catalyst retained its activity for 18 h. The rate of methane conversion was low (0.7 – 1.0 mmol CH_4 g_{cat}^{-1} h^{-1}).

An example of a faster (200 mmol CH_4 g_{cat}^{-1} h^{-1}) selective Non-OCM reaction on ZSM-5 zeolite-supported Pt – Bi catalyst (Pt – Bi/ZSM-5) at 600 – 700 °C to give the C_2 hydrocarbons with high selectivity (> 90%) and dominant formation of ethane was reported.[31] The conversion of methane attained equilibrium values (2% – 3%). Based on experimental observations, it was assumed that activation of methane proceeds at the platinum sites, while the bismuth promoter plays an important role in the formation of the C_2 species.

Lukyanov and Vazhnova [341] established that the zeolite component of the catalyst also contributes largely to the steady-state course of the Non-OCM reaction on a platinum-containing zeolite at moderate temperatures. The conversion of methane to ethane on the Pt – ZSM-5 zeolite at 370 °C proceeded with a C_2H_6 selectivity of more than 95%, although the conversion of methane was low (~0.17%), being limited by the equilibrium conditions.[16] The catalyst lifetime was longer than 28 h. Another platinum catalyst, Pt/Al_2O_3, showed a low activity under identical conditions and rapidly deactivated.

A direct conversion of methane to ethylene on titanium hybrid systems at relatively low temperatures was demonstrated.[342, 343] At 450 °C and a pressure of 1 MPa, ethylene was obtained with a selectivity of nearly 50% at a CH_4 conversion in the range of 15% – 20%.

Experimental data obtained by different research groups [30, 31, 341 – 343] are indicative of efficient activation of methane on zeolite-containing catalysts and on titanium hybrid systems at moderate temperatures (370 – 650 °C) and of the possibility of selective production of C_2 hydrocarbons by the Non-OCM reaction. However, thermodynamic constraints [16] prohibit carrying out the process with high conversion at moderate temperatures. Practically admissible yields of C_2 hydrocarbons can be obtained by direct conversion of methane only at temperatures above 900 °C.[16]

It was found that single iron active sites embedded into a silica matrix Fe@SiO_2 can efficiently catalyze selective conversion of methane to ethylene at 1000 – 1100 °C.[344] The absence of adjacent iron sites prevents catalytic coupling of C – C units formed in the initial stage, their subsequent oligomerization and coke deposition. The ethylene selectivity is as high as 45% – 48%. Other reaction products include benzene (selectivity ~30%) and naphthalene (selectivity ~25%). At 1090 °C, the methane conversion takes a maximum value of 48%. Ethylene was obtained in 25% yield. The reaction proceeds as a steady-state process. The catalyst lifetime is longer than 60 h.

Yet another study [345] was carried out to assess the prospects for conducting a Non-OCM reaction on Fe@SiO_2 catalyst in a membrane reactor with a hydrogen-permeable membrane. The tubular membrane reactor represented a mixed ionic-electronic $SrCe_{0.7}Zr_{0.2}Eu_{0.1}O_{3-\delta}$ thin film supported on the outer surface of a porous $SrCe_{0.8}$ $Zr_{0.2}O_{3-\delta}$ tube. Attempts were made to shift the equilibrium in the Non-OCM reaction and to increase the conversion of methane through removal of H_2 from the reaction section.

Researchers at Sasol studied an alternative, catalyst-free, pathway of the non-OCM reaction in a microwave plasma reactor.[346] The conversion of methane to hydrocarbons under low-temperature plasma conditions was 15% with an ethane selectivity of 60%. As the temperature of the gas increases, the conversion increases, but the selectivity is shifted towards the formation of acetylene and coke deposits. This limits the yield of ethylene to 7% – 8%.

Thus, the process on the Fe@SiO_2 catalyst seems to be the most promising version of the Non-OCM reaction. However, its possible commercialization is hampered by the high reaction temperature, which implies large energy expenditure.

9. Conclusion

Various methods for conversion of methane to lower olefins are available. Now we will compare certain characteristics of the most efficient methods that may appear to be of interest to not only researchers, but also industry. Most new methods for the synthesis of ethylene and propylene are at least competitive with the industrial production of olefins by pyrolysis of naphtha in efficiency of conversion of hydrocarbon raw material (Table 10). Compared to traditional technologies, the alternative methane-based processes better meet the requirements of global 'olefin' market to ensure the production of olefins in the ratio $C_3^= : C_2^= \geqslant 0.6$ (in connection with increasing propylene deficiency).[8, 53] Methods for conversion of methane to olefins differ in number of stages, range of products, possibility of integration into industrial production cycles, thermal load distribution and some other parameters (see Table 10).

Multistage methods (MTO, MTP, DTO) are characterized by more uniform thermal load distribution, high conversion of methane (70% – 90%), wide range of value-added products (olefins, methanol and/or DME) and the possibility to vary the propylene : ethylene ratio in the 'olefin' product (see Table 10). Taken altogether, these features make the production 'tunable' and economically stable and allow the methanol and DME markets to correlate with the olefin (polyolefin) markets. Recent extensive construction of large-scale plants for the synthesis of olefins *via* methanol shows that these processes are of interest to industry and investors.

Other methods for production of lower olefins from methane (FTSO, OX – ZEO, MCTO, OCM, Non-OCM) involve a smaller number of stages than the MTO, MTP and DTO processes but seem to be less attractive from the standpoint of range of products. Nevertheless, they are also aimed at integrating into the existing production cycles and, therefore, are of practical interest and can, in the future, carve out a relevant niche in natural gas chemical industry.

Successful commercialization of certain 'methane' processes began at Honeywell (UOP), Lurgi, DICP, *etc*. However, considerable efforts are required to industrialize most of them as complete alternative to pyrolysis of naphtha.

In spite of a wide variety of methods for the synthesis of olefins from methanol, DME, methyl chloride, syngas, or directly from methane, some general trends in their development can be distinguished. High efficiency of all methods for production of ethylene (propylene) from methane is to a great extent due to the use of various design features.

Table 10. Characteristics of main modern methods for methane conversion to lower olefins.

Method (development company)	Thermal load distribution over main reaction stages			Yield on carbon basis (%)		Target products	$C_3^=$: $C_2^=$ (see [b])	Problematic side products	Possibility to integrate with full-scale production	Ref.
	reaction stage	T /°C	ΔH°_{298} /kJ mol^{-1}	single-pass	total [a]					
MTO – OCP (Hoheywell (UOP)/Total)	1. Methane reforming (autothermal)	800	+146	–	85 – 90	Ethylene, propylene, methanol	0.7 – 1.8	–	With methanol production	43, 44
	2. Synthesis of methanol	260	−92	–						
	3. Methanol conversion to olefins + cracking of $C_{4+}^=$ olefins	450	−30 (see [c])	70 – 80						
MTP (Lurgi)	1. Methane reforming (autothermal)	800	+146	–	65 – 70	Propylene, gasoline, DME, methanol	> 70	–	With methanol production	45,46
	2. Synthesis of methanol	260	−92	–						
	3. Methanol dehydration to DME	380	−23	–						
	4. Conversion of methanol + DME + water mixture to olefins	450	−17 (see [c])	20 – 50						
DTO (TIPS RAS)	1. Methane reforming (autothermal)	800	+146	–	> 80	Ethylene, propylene, DME	1.0 – 1.5	CO_2 (see [d])	With DME production	71
	2. Synthesis of methanol	280	−207	–						
	3. DME conversion to olefins	340	−4 (see [c])	> 80						
FTSO (Beijing University ChemTech)	1. Methane reforming (autothermal)	800	+146	–	–	Ethylene, propylene, fuel hydrocarbons	1.0 – 1.3	CO_2, CH_4	With diesel production	209
	2. Syngas conversion to olefins	350	−211 (see [c])	38 – 43						
OX – ZEO (DICP, Xiamen University)	1. Methane reforming (autothermal)	800	+146	–	–	Ethylene, propylene, fuel hydrocarbons	0.6 – 1.3	CO_2, CH_4	With diesel production	242, 247
	2. Syngas conversion to olefins	400	−211 (see [c])	14 – 21						
MCTO (OOO 'Sintez')	1. Oxidative chlorination of methane to methyl chloride	300	−162	–	to 70	Ethylene, propylene, dichloroethane	0.8	Chlorine-containing products	With chlorine production	268
	2. Methyl chloride conversion to olefins	450	+42 (see [c])	55 – 65						
OCM (Siluria)	1. Partial oxidation of methane by oxygen to ethylene – ethane mixture	550	−266 (see [c])	14 – 20	71	Ethylene	0.04	CO_2, CO, CH_4 (see [e])	With liquefied gas production, with pyrolysis of ethane	322

Table 10 (continued).

Method (development company)	Thermal load distribution over main reaction stages			Yield on carbon basis (%)		Target products	$C_3^= : C_2^=$ (see [b])	Problematic side products	Possibility to integrate with full-scale production	Ref.
	reaction stage	T/°C	ΔH°_{298} /kJ mol^{-1}	single-pass	total [a]					
OCM (Russian research centres)	1. Partial oxidation of methane by oxygen to ethylene – ethane mixture	800 – 1000	−266 (see [c])	15 – 16	–	Ethylene	–	CO_2, CO, CH_4	With liquefied gas production, with pyrolysis of ethane	288, 291, 297
Non-OCM (DICP)	1. Non-oxidative coupling of methane	1090	+ 65 (see [c])	25	–	Ethylene, aromatic hydrocarbons	–	Coke	With liquefied gas production, with pyrolysis of ethane	344
Pyrolysis of naphtha (for comparison)	1. Pyrolysis of naphtha	800 – 1000	–	–	70	Ethylene, propylene, gasoline	0.4	–	–	293

[a] For the overall process (taking account of all techniques used).
[b] In accordance with requirements of modern olefin market, $C_3^= : C_2^= > 0.6$.[8, 53]
[c] Calculated per mol of ethylene.
[d] Recycle of CO_2 per methane reforming stage.
[e] Methanation of carbon oxides, recycle of methane.

Considering the synthesis of olefins, in almost all cases the single-pass yield of olefins is low while the activity and selectivity of catalysts are insufficiently high (see Table 10). Most researchers widely use hybrid catalysts containing the shape selective zeolite component (SAPO-34, ZSM-5, *etc.*) and begin to utilize nanosized catalytic systems. Besides, various innovative technologies were proposed, including new-generation (membrane, Berty) reactors; three-phase systems, *etc.*; multistage, one-pot procedures; methods for CO_2 recovery (CO_2 is the major side product of certain processes), *etc*.

We believe the achievements in a certain method can be transferred to other ones to create prerequisites for progress in other methods for methane processing to olefins. For instance, methods for the preparation of nanosized catalytic systems and productive recovery of carbon dioxide, the experience in the application of zeolites and some innovative technological features may appear to be common to different processes.

The authors hope the results obtained by different research groups and generalized in this review will help chemists working in the field of deep conversion of natural gas to lower olefins with further planning of their activity taking account of all innovations and advances in related research areas.

Figures 1 and 5 were compiled by the authors of this review using the data taken from certain original publications (for corresponding references, see captions).

Figures 3 and 4 are courtesy of MDPI AG.

This review has been written within the framework of the State Assignment to TIPS RAS.

References

1. S.A.Nikolaev, V.V.Smirnov, L.N.Zanaveskin, K.L.Zanaveskin, V.A.Averyanov. *Russ. Chem. Rev.*, **78**, 231 (2009)
2. S.M.Sadrameli. *Fuel*, **173**, 285 (2016)
3. V.A.Men'shikov, M.Yu.Sinev. *Katalis v Promyshlennosti*, **1**, 25 (2005)
4. *The Ethylene Technology Report 2016*. In *US Energy Inf. Administr., Int. Energy Outlook 2016* (2016)
5. R.Brown. *Chem. Mark. Rep.*, **261**, 1 (2002)
6. N.Chikamatsu, K.Honda, A.Okita, J.Takahashi, K.Oyama, M.Nakamura. In *7th Asian DME Conf., Niigata, Japan.* (Nov. 2011) [https://docplayer.net/101512204-Dominant-technology-for-thepropylene-production-dtp-r-process.html (Last accessed 27.01.2020)]
7. V.S.Arutyunov, G.V.Lisichkin. *Russ. Chem. Rev.*, **86**, 777 (2017)
8. I.Amghizar, L.A.Vandewalle, K.M.van Geem, G. B. Marin. *Engineering*, **3**, 171 (2017)
9. *Natural Gas Opportunity*. [http://siluria.com/Feedstock/Natural_Gas_Opportunity (Last accessed 27.01.2020)]
10. R.S.Yarullin. In. *X Moskovskii Mezhdunarodnyi Khimicheskii Sammit, 7 – 8 Oktyabrya, 2014* (The Xth Moscow International Chemical Summit, 7 – 8 October, 2014) [http://www.chemsummit.ru/wp-content/uploads/2014/10/8_regiony_Yarullin_10-chemsummit.pdf (Last accessed 27.01.2020)]
11. E.V.Kondratenko, T.Peppel, D.Seeburg, V.A.Kondratenko, N.Kalevaru, A.Martin, S.Wohlrab. *Catal. Sci. Technol.*, **7**, 366 (2017)
12. P.Schwach, X.Pan, X.Bao. *Chem. Rev.*, **117**, 8497 (2017)
13. D.A.Wood. *J. Nat. Gas Sci. Eng.*, **26**, 780 (2015)
14. S.M.Aldoshin, V.S.Arutyunov, V.I.Savchenko, I.V.Sedov. *Neftesazokhimiya*, **3**, 60 (2015)
15. Y.Gambo, A. A.Jalil, S.Triwahyono, A.A.Abdulrasheed. *J. Ind. Eng. Chem.*, **59**, 218 (2018)
16. C.Karakaya, R.J.Kee. *Prog. Energ. Combust.*, **55**, 60 (2016)
17. A.I.Olivos-Suarez, A.Szécsényi, E.J.M.Hensen, J.Ruiz-Martinez, E.A.Pidko, J.Gascon. *ACS Catal.*, **6**, 2965 (2016)
18. A.Galadima, O.Muraza. *J. Ind. Eng. Chem.*, **37**, 1 (2016)
19. M.Khanmohammadi, Sh.Amani, A.B.Garmarudi, A.Niaei. *Chin. J. Catal.*, **37**, 325 (2016)
20. P.Tian, Y.Wei, M.Ye, Z.Liu. *ACS Catal.*, **5**, 1922 (2015)
21. U.Olsbye, S.Svelle, M.Bjurgen, P.Beato, T.V.W.Janssens, F.Joensen, S.Bordiga, K.P.Lillerud. *Angew. Chem., Int. Ed.*, **51**, 5810 (2012)
22. U.Olsbye, S.Svelle, K.P.Lillerud, Z.H.Wei, Y.Y.Chen, J.F.Li, J.G.Wang, W.B.Fan. *Chem. Soc. Rev.*, **44**, 7155 (2015)
23. H.Schulz. *Catal. Today*, **154**, 183 (2010)
24. J.S.Martinez-Espin, M.Mortén, T.V.W.Janssens, S.Svelle, P.Beato, U.Olsbye. *Catal. Sci. Technol.*, **7**, 2700 (2017)
25. M.Ye, H.Li, Y.Zhao, T.Zhang, Zh.Liu. *Adv.Chem. Eng.*, **47**, 279 (2015)
26. S.N.Khadzhiev, M.V.Magomedova, E.G.Peresypkina. *Petrol. Chem.*, **54**, 245 (2014)
27. S.N.Khadzhiev, N.V.Kolesnichenko, N.N.Ezhova. *Petrol. Chem.*, **48**, 326 (2008)
28. P.T.D.Batamack, Th.Mathew, G.K.S.Prakash. *J. Am. Chem. Soc.*, **139**, 18078 (2017)
29. V.N.Rozanov, Yu.A.Treger, O.P.Murasheva, I.S.Silina, E.A.Avarina. *Nwftegazokhimiya*, **3**, 69 (2015)
30. H.Sheng, E.P.Schreiner, W.Zheng, R.F.Lobo. *ChemPhysChem*, **19**, 504 (2018)
31. Y.Xiao, A.Varma. *ACS Catal.*, **8**, 2735 (2018)
32. J.Zhang, N.Wei, H.Zhong, Y.Zhou, L.Pan. *Chem. Phys. Lett.*, **714**, 74 (2019)
33. D.Pashchenko. *Fuel*, **236**, 686 (2019)
34. A.S.Brayko, A.B.Shigarov, V.A.Kirillov, V.V.Kireenko, N.A.Kuzin, V.A.Sobyanin, P.V.Snytnikov, V.V.Kharton. *Mater. Lett.*, **236**, 264 (2019)
35. I.V.Zagaynov, A.S.Loktev, I.E.Mukhin, A.G.Dedov, I.I.Moiseev. *Mendeleev Commun.*, **27**, 509 (2017)
36. W.J.Jang, J.O.Shim, H.M.Kim, S.Y.Yoo, H.S.Roh. *Catal. Today*, **324**, 15 (2019)
37. M.Luneau, E.Gianotti, N.Guilhaume, E.Landrivon, F.C.Meunier, C.Mirodatos, Y.Schuurman. *Ind. Eng. Chem. Res.*, **56**, 13165 (2017)
38. S.Sepehri, M.Rezaei, G.Garbarino, G.Busca. *Int. J. Hydr. Energy,* **41**, 8855 (2016)
39. H.Ryoo, B.Ch.Ma, Y.Ch.Kim. *J. Nanosci. Nanotechnol.*, **19**, 988 (2019)
40. H.T.Luk, C.Mondelli, D.C.Ferre, J.A.Stewart, J.Perez-Ramirez. *Chem. Soc. Rev.*, **46**, 1358 (2017)
41. A.K.Chernyshev, V.A.Daut, A.K.Surba, A.V.Sirotin, V.Ya.Kunitskii, V.N.Mikhlai, M.V.Tataryshkin, K.A.Chernyshev. *Metanol: Svoistva, Proizvodstvo, Primenenie*. (Methanol: Properties, Production and Application). Vol. II. (Moscow: Infokhim, 2011)
42. S.Jasper, M.M.El-Halwagi. *Processes*, **3**, 684 (2015)
43. Patent US 7317133 (2002)
44. P.Barger. *Catal. Sci. Ser.*, **3**, 239 (2002)
45. Patent US 7015369 (2006)
46. H.Koempel, W.Liebner. In *Proceeding 8th Natural Gas Conversion Symposium*, (Natal, Brazil. 2007). P. 261
47. Patent US 7371915 (2008)
48. Patent EP 006851 (2006)
49. Patent US 7393990 (2008)
50. B.V.Vora, T.L.Marker, P.T.Barger, H.R.Nilsen, S.Kvisle, T.Fuglerud. *Stud. Surf. Sci. Catal.*, **107**, 87 (1997)
51. J.Gregor. *Methanol to Olefins. A Pillar of Capacity Additions in China, but does MTO have a Role in India*? IOCL Conclave. Feb. 7, 2014. UOP LLC Des Plaines, Illinois, USA [www.petrochemconclave.com/presentation/2014/Mr.JGregor.pdf (Last accessed 27.01.2020)]
52. X.Xu, Y.Liu, F.Zhang, W.Di, Y.Zhang. *Catal. Today*, **298**, 61 (2017)

53. J.S.Plotkin. *The Propylene Gap: How can it be Filled?* (Washington, DC: American Chemical Society, 2015)
54. C.Li, J.Li, J.Li, H.Yu. *Chem. Ind. Eng. Prog.*, **29**, 315 (2010)
55. Patent US 6399844 (2002)
56. R.Xu, B.Zhang, Y.Zhang, G.Liu, X.Hao, Y.Chen. *Nat. Gas Chem. Ind.*, **41**, 81 (2016)
57. S.Gao, S.Hu, Y.Wei, Q.Qiao, Z.Xu, X.Wu, M.Zhang, Y.He, S.Xu, Z.Liu. *J. Catal.*, **367**, 306 (2018)
58. Ch.Vogt, B.M.Weckhuysen, J.Ruiz-Martinez. *ChemCatChem*, **9**, 183 (2017)
59. E.C.Nordvang, E.Borodina, J.Ruiz-Martinez, R.Fehrmann, B.M.Weckhuysen. *Chem. – Eur. J.*, **21**, 17324 (2015)
60. Y.Zhang, M.Li, E.Xing, Y.Luo, X.Shu. *Catal. Commun.*, **119**, 67 (2019)
61. S.V.Konnov, V.S.Pavlov, P.A.Kots, V.B.Zaytsev, I.I.Ivanova. *Catal. Sci. Technol.*, **6**, 1564 (2018)
62. D.M.Brown, B.L.Bhatt, T.H.Hsiung, J.J.Lewnard, F.J.Waller. *Catal. Today*, **8**, 279 (1991)
63. M.R.Gogate. *Petrol. Sci. Technol.*, **36**, 562 (2018)
64. A.S.Al-Dughaither, H. Lasa. *Fuel*, **138**, 52 (2014)
65. S.N.Khadzhiev, N.N.Ezhova, O.V.Yashina. *Petrol. Chem.*, **57**, 553 (2017)
66. Patent US 6852897 (2005)
67. G.Cai, Z.Liu, R.Shi, Ch.He, L.Yang, Ch.Sun, Y.Chang. *Appl. Catal. A: Gen.*, **125**, 29 (1995)
68. Patent RU 2220939 (2003)
69. Patent RU 2218988 (2003)
70. Patent RU 2323777 (2008)
71. N.V.Kolesnichenko, T.I.Goryainova, E.N.Biryukova, O.V.Yashina, S.N.Khadzhiev. *Petrol. Chem.*, **51**, 55 (2011)
72. Y.Ohno, M.Yoshida, T.Shikada, O.Inokoshi, T.Ogawa, N.Inoue. *JFE Technical Report. Í 8. October 2006*. [www.jfe-steel.co.jp/en/research/report/008/pdf/008-06.pdf (Last accessed 27.01.2020)]
73. N.V.Kolesnichenko, N.N.Ezhova, A.N.Stashenko, A.E.Kuzmin, O.V.Yashina, K.B.Golubev. *Russ. J. Appl. Chem.*, **91**, 1773 (2018)
74. N.V.Kolesnichenko, O.V.Yashina, N.N.Ezhova, G.N.Bondarenko, S.N.Khadzhiev. *Russ. J. Phys. Chem. A*, **92**, 118 (2018)
75. J.S.Martinez-Espin, K.de Wispelaere, M.Westgúrd Erichsen, S.Svelle, T.V.W.Janssens, V.van Speybroeck, P.Beato, U.Olsbye. *J. Catal.*, **349**, 136 (2017)
76. S. Svelle, S.Kolboe, O.Swang, U.Olsbye. *J. Phys. Chem. B*, **109**, 12874 (2005)
77. X.Sun, S.Müller, Y.Liu, H.Shi, G.L.Haller, M.Sanchez-Sanchez, A.C.Van Veen, J.A.Lercher. *J. Catal.*, **317**, 185 (2014)
78. S.Müller, Y.Liu, F.M.Kirchberger, M.Tonigold, M.Sanchez-Sanchez, J.A.Lercher. *J. Am. Chem. Soc.*, **138**, 15994 (2016)
79. J.Gil-Coba, S.C.Marie-Rose, J.M.Lavoie. *Catal. Lett.*, **146**, 2534 (2016)
80. M.Ghavipour, R.M.Behbahani, R.B.Rostami, A.S.Lemraski. *J. Nat. Gas Sci. Eng.*, **21**, 532 (2014)
81. M.H.M.Ahmed, O.Muraza, A.M.Al-Amer, K.Miyake, N.Nishiyama. *Appl. Catal., A*, **497**, 127 (2015)
82. M.H.M.Ahmed, O.Muraza, A.M.Al-Amer, Y.Sugiara, N.Nishiyama. *Microporous Mesoporous Mater.*, **207**, 9 (2015)
83. P.Pérez-Uriarte, A.Ateka, A.T.Aguayo, J.Bilbao. *Catal. Lett.*, **146**, 1892 (2016)
84. P.Pérez-Uriarte, A.Ateka, A.T.Aguayo, A.G.Gayubo, J.Bilbao. *Chem. Eng. J.*, **302**, 801 (2016)
85. J.Li, Z.Wei, Y.Chen, B.Jing, Y.He, M.Dong, H. Jiao, X.Li, Z.Qin, J.Wang, W.Fan. *J. Catal.*, **317**, 277 (2014)
86. Y.Li, M.Zhang, D.Wang, F.Wie, Y.Wang. *J. Catal.*, **311**, 281 (2014)
87. Y.Hirota, K.Murata, M.Miyamoto, Y.Egashira, N.Nishiyama. *Catal. Lett.*, **140**, 22 (2010)
88. Y.Hirota, M.Yamada, Y.Uchida, Y.Sakamoto, T.Yokoi, N.Nishiyama. *Microporous Mesoporous Mater.*, **232**, 65 (2016)
89. D.Zhao, Y.Zhang, Z.Li, Y.Wang, J.Yu. *RSC Adv.*, **7**, 939 (2017)
90. B.Zhao, H.Zhang, Z.Li, Y.Wang, J.Yu. *Chem. Eng. J.*, **323**, 295 (2017)
91. G.Nasser, T.Kurniawan, K.Miyake, A.Galadima, Y.Hirota, N.Nishiyama, O.Muraza. *J. Nat. Gas Sci. Eng.*, **28**, 566 (2016)
92. Y.Wang, J.Li, W.Mi. *React. Kinet. Catal. Lett.*, **76**, 141 (2002)
93. R.Wendelbo, D.Akporiaye, A.Andersen, I.M.Dahl, H.B.Mostad. *Appl. Catal., A*, **142**, L197 (1996)
94. B.P.C.Hereijgers, F.Bleken, M.H.Nilsen, S.Svelle, K.P.Lillerud, M.Bjorgen, B.M.Weckhuysen, U.Olsbye. *J. Catal.*, **264**, 77 (2009)
95. J.Zhu, Y.Li, U.Muhammad, D.Wang, Y.Wang. *Chem. Eng. J.*, **316**, 187 (2017)
96. A.Hwang, T.T.Le, Z.Shi, H.Dai, J.D.Rimer, A.Bhan. *J. Catal.*, **369**, 122 (2019)
97. S.Aghamohammadi, M.Haghighi. *Adv. Powder Technol.*, **27**, 1738 (2016)
98. G.J.Yang, Y.X.Wei, S.T.Xu, J.R.Chen, J.Z.Li, Z.M.Li, J.H.Yu, R.R.Xu. *J. Phys. Chem. C*, **117**, 8214 (2013)
99. J.Wu, Z.Y.Liu, L.Xia, M.H.Qiu, X.Liu, H.J.Zhu, Y.H.Sun. *Chin. J. Catal.*, **34**, 348 (2013)
100. H.E.van der Bij, B.M.Weckhuysen. *Phys. Chem. Chem. Phys.*, **16**, 9892 (2014)
101. J.Zhong, J.Han, Y.Wei, P.Tian, X.Guo, C.Song, Z.Liu. *Catal. Sci. Technol.*, **21**, 4905 (2017)
102. H.S.Pajaie, M.Taghizadeh. *React. Kinet. Mech. Catal.*, **118**, 701 (2016)
103. Y.Zhang, Z.Ren, Y.Wang, Y.Deng, J.Li. *Catalysts*, **8**, 570 (2018)
104. H.J.Chae, Y.H.Song, K.E.Jeong, C.U.Kim, S.Y.Jeong. *J. Phys. Chem. Solids*, **71**, 600 (2010)
105. L.Li, X.Cui, J.Li, J.Wang. *J. Braz. Chem. Soc.*, **26** (2), 290 (2015)
106. J.Chen, J.Li, Y.Wei, C.Yuan, B.Li, S.Xu, Y.Zhou, J.Wang, M.Zhang, Z.Liu. *Catal. Commun.,* **46**, 36 (2014)
107. J.Zhu, Y.Cui, Z.Nawaz, Y.Wang, F.Wei. *Chin. J. Chem. Eng.*, **18**, 979 (2010)
108. S.G.Lee, H.S.Kim, Y.H.Kim, E.J.Kang, D.H.Lee, C.S.Park. *J. Ind. Eng. Chem.*, **20**, 61 (2014)
109. M.Fujiwara, N.Mimura, O.Sato, A.Yamaguchi. *Microporous Mesoporous Mater.*, **280**, 219 (2019)
110. T.S.Zhao, T.Takemoto, N.Tsubaki. *Catal. Commun.*, **7**, 647 (2006)
111. I.A.Bakare, O.Muraza, M.A.Sanhoob, K.Miyake, Y.Hirota, Z.H.Yamani, N.Nishiyama. *Fuel*, **211**, 18 (2018)
112. E.E.Kolesnikova, T.K.Obukhova, N.V.Kolesnichenko, G.N.Bondarenko, O.V.Arapova, S.N.Khadzhiev. *Petrol. Chem.*, **58**, 863 (2018)
113. T.I.Goryainova, E.N.Biryukova, N.V.Kolesnichenko, S.N.Khadzhiev. *Petrol. Chem.*, **51**, 169 (2011)
114. M.V.Magomedova, E.G.Peresypkina, I.A.Davydov, S.N.Khadzhiev. *Petrol. Chem.*, **57**, 1043 (2017)
115. N.V.Kolesnichenko, V.S.Pavlov, A.N.Stashenko, O.V.Yashina, N.N.Ezhova, S.V.Konnov, S.N.Khadzhiev. *React. Kinet. Mech. Catal.*, **124**, 1 (2018)
116. N.V.Kolesnichenko, O.V.Yashina, N.A.Markova, E.N.Biryukova, T.I.Goryainova, R.V.Kulumbegov, S.N.Khadzhiev, L.E.Kitaev, V.V.Yuschenko. *Petrol. Chem.*, **49**, 42 (2009)
117. E.E.Kolesnikova, L.E.Kitaev, E.N.Biryukova, N.V.Kolesnichenko, S.N.Khadzhiev. *Petrol. Chem.*, **53**, 33 (2013)
118. E.N.Khivrich, T.I.Batova, E.E.Kolesnikova, N.V.Kolesnichenko. *Khim. Prom. Segodnya*, (6), 9 (2014)

119. Patent RU 2518091 (2014)
120. N.V.Kolesnichenko, E.E.Kolesnikova, T.K.Obuchova, G.N.Bondarenko. *Petrol. Chem.*, **58**, 1013 (2018)
121. M.Rostamizadeh, A.Taeb. *J. Ind. Eng. Chem.*, **27**, 297 (2015)
122. Y.Song, L.L.Zhang, G.D.Li, Y.S.Shang, X.M.Zhao, T.Ma, L.M.Zhang, Y.L.Zhai, Y.J.Gong, J.Xu, F.Deng. *Fuel Proc. Technol.*, **168**, 105 (2017)
123. X.Zhao, Y.Hong, L.Wang, D.Fan, N.Yan, X.Liu, P.Tian, X.Guo, Z.Liu. *Chin. J. Catal.*, **39**, 418 (2018)
124. S.F.Zhao, X.T.Yao, B.H.Yan, L.Li, Y.M.Liu, M.Y.He. *Chin. Chem. Lett.*, **28**, 1318 (2017)
125. P.Losch, M.Boltz, C.Bernardon, B.Louis, A.Palčić, V.Valtchev. *Appl. Catal., A*, **509**, 30 (2016)
126. I.Yarulina, K.de Wispelaere, S.Bailleul, J.Goetze, M.Radersma, E.Abou-Hamad, I.Vollmer, M.Goesten, B.Mezari, E.J.M.Hensen, J.S.Martinez-Espin, M.Morten, Sh.Mitchell, J.Perez-Ramirez, U.Olsbye, B.M.Weclhuysen, V.van Speybroeck, F.Kapteijin, J.Gascon. *Nat. Chem.*, **10**, 804 (2018)
127. X.Li, F.Rezaei, A.Rownaghi. *Microporous Mesoporous Mater.*, **276**, 1 (2019)
128. N.Hadi, A.Niaei, S.R.Nabavi, A.Farzi, M.N.Shirazi. *Chem. Biochem. Eng. Q*, **28**, 53 (2014)
129. N.Hadi, A.Niaei, S.R.Nabavi, R.Alizadeh, M.N.Shirazi, B.Izadkhah. *J. Taiwan Ins. Chem. Eng.*, **59**, 173 (2016)
130. H.R.Zhang, Z.X.Ning, J.P.Shang, H.Y.Liu, S.H.Han, W.S.Qu, Y.Jiang, Y.Guo. *Microporous Mesoporous Mater.*, **248**, 173 (2017)
131. H.Zhang, Z.Ning, H.Liu, J.Shang, S.Han, D.Jiang, Y.Jiang, Y.Guo. *RSC Adv.,* **7**, 16602 (2017)
132. T.I.Batova, E.N.Khivrich, G.N.Shirobokova, N.V.Kolesnichenko, Yu.V.Pavlyuk, G.N.Bondarenko. *Petrol. Chem.*, **53**, 383 (2013)
133. T.Cordero-Lanzac, A.Ateka, P.Pérez-Uriarte, P.Castaco, A.T.Aguayo, J.Bilbao. *Ind. Eng. Chem. Res.*, **57**, 13689 (2018)
134. P.Perez-Uriarte, M.Gamero, A.Ateka, A.T.Aguayo, J.Bilbao. *Ind. Eng. Chem. Res.*, **55**, 6569 (2016)
135. P.Perez-Uriarte, A.Ateka, A.G.Gayubo, T.Cordero-Lanzac, A.T.Aguayo, J.Bilbao. *Chem. Eng. J.*, **311**, 367 (2017)
136. L.Tosheva, V.Valtchev. *Chem. Mater.*, **17**, 2494 (2005)
137. V.Valtchev, L.Tosheva. *Chem. Rev.*, **113**, 6734 (2013)
138. T.Taniguchi, K.Yoneta1, S.Nakaoka, Y.Nakasaka, T.Yokoi, T.Tago, T.Masuda. *Catal. Lett.*, **146**, 442 (2016)
139. M.Rahmani, M.Taghizadeh. *React. Kinet. Mech. Catal.*, **122**, 409 (2017)
140. K.Y.Lee, S.W.Lee, S.K.Ihm. *Ind. Eng. Chem. Res.*, **53**, 10072 (2014)
141. P.Losch, A.B.Pinar, M.G.Willinger, K.Soukup, S.Chavan, B.Vincent, P.Pale, B.Louis. *J. Catal.*, **345**, 11 (2017)
142. P.Losch, M.Boltz, B.Louis, S.Chavan, U.Olsbye. *Compt. Rend. Chim.*, **18**, 330 (2015)
143. J.Li, M.Liu, X.Guo, C.Dai, C.Song. *J. Energy Chem.*, **27**, 1225 (2018)
144. M.Khatamian, A.Yavari, A.Akbarzadeh, E.Alizadeh. *Mater. Sci. Eng. C*, **78**, 1212 (2017)
145. R.Qi, T.Fu, W.Wan, Z.Li. *Fuel Proc. Technol.*, **155**, 191 (2017)
146. R.Feng, X.Wang, J.Lin, Z.Li, K.Hou, X.Yan, X.Hu, Z.Yan, M.J.Rood. *Microporous Mesoporous Mater.*, **270**, 57 (2018)
147. R.Feng, X.Yan, X.Hu, Z.Yan, J.Lin, Z.Li, M.J.Rood. *Catal. Commun.*, **109**, 1 (2018)
148. H.Chen, Y.Wang, Ch.Sun, F.Gao, L.Sun, C.Wang, Zh.Wang, X.Wang. *Catal. Commun.*, **100**, 107 (2017)
149. H.Chen, Y.Wang, C.Sun, X.Wang, C.Wang. *Catal. Commun.*, **112**, 10 (2018)
150. H.Chen, Y.Wang, F.Meng, C.Sun, H.Li, Z.Wang, F.Gao, X.Wang, S.Wang. *Microporous Mesoporous Mater.*, **244**, 301 (2017)
151. Y.Sang, A.Xing, C.Wang, Z.Han, Y.Wu. *Catalysts*, **7**, 171 (2017)
152. M.Rostamizadeh, A.Taeb. *Synth. React. Inorg. Metal-Org. Nano-Metal Chem.*, **46**, 665 (2016)
153. N.Hadi, R.Alizadeh, A.Niaei. *J. Ind. Eng. Chem.*, **54**, 82 (2017)
154. Y.Shang, W.Wang, Y.Zhai, Y.Song, X.Zhao, T.Ma, J.Wei, Y.Gong. *Microporous Mesoporous Mater.*, **276**, 173 (2019)
155. L.Wang, Z.Wang, H.Q.Jiao, X.J.Yong, C.T.Luo, D.H.Liu. *China Petrol. Proc. Petrochem. Technol.*, **20**, 8 (2018)
156. F.Yaripour, Z.Shariatinia, S.Sahebdelfar, A.Irandoukht. *Microporous Mesoporous Mater.*, **203**, 41 (2015)
157. Y.Jiao, X.Yang, C.Jiang, C.Tian, Z.Yang, J.Zhang. *J. Catal.*, **332**, 70 (2015)
158. A.E.Persson, B.J.Schoeman, J.Sterte, J.E.Otterstedt. *Zeolites*, **15**, 611 (1995).
159. R.van Grieken, J.L.Sotelo, J.M.Meneündez, J.A.Melero. *Microporous Mesoporous Mater.*, **39**, 135 (2000)
160. Patent EP 173901 (1986)
161. Patent US 4205053 (1979)
162. Patent US 3781226 (1972)
163. Patent US 3926782 (1973)
164. Patent US 4526879 (1978)
165. Y.Liu, W.Zhang, Z.Liu, S.Xu, Y.Wang, Z.Xie, X.Han, X.Bao. *J. Phys. Chem. C.*, **112**, 15375 (2008)
166. S.Inagaki, S.Shinoda, Y.Kaneko, K.Takechi, R.Komatsu, Y.Tsuboi, H.Yamazaki, J.N.Kondo, Y.Kubota. *ACS Catal.*, **3**, 74 (2013)
167. D.P.Serrano, R.Grieken. *J. Mater. Chem.*, **11**, 2391 (2001)
168. R.Ravandi, R.Khoshbin, R.Karimzadeh. *J. Porous Mater.,* **25**, 451 (2018)
169. E.Mohiuddin, Y.Makarfi. *Appl. Clay Sci.*, **119**, 231 (2016)
170. H.Liu, T.Shen, T.Li, P.Yuan, G.Shi, X.Bao. *Appl. Clay Sci.*, **90**, 53 (2014)
171. Y.Li, H.Sun, R.Feng. *Appl. Petrochem. Res.,* **5**, 347 (2015)
172. W.Yu, L.Deng, P.Yuan, D.Liu, W.Yuan, F.Chen. *Chem. Eng. J.*, **270**, 450 (2015)
173. Y.Wang, Y.Chang, M.Liu, A.Zhang, C.Song, X.Guo. *Preprints*, 2017040009, 2017 (doi: 10.20944/preprints201704.0009.v1)
174. Patent US 4257885 (1981)
175. G.Majano, A.Darwiche, S.Mintova, V.Valtchev. *Ind. Eng. Chem. Res.*, **48**, 7048 (2009)
176. H.Zhang, Y.Ma, K.Song, Y.Zhang, Y.Tang. *J. Catal.*, **302**, 115 (2013)
177. G.Wu, W.Wu, X.Wang, Z.Wang, W.Wang. *Microporous Mesoporous Mater.*, **180**, 187 (2013)
178. K.Zhang, S.A.Kurumov, X.Su, Y.M.Snatenkova, Z.M.Bukina, N.V.Kolesnichenko, W.Wu, S.N.Khadzhiev. *Petrol. Chem.*, **57**, 1036 (2017)
179. C.J.H.Jacobsen, C.Madsen, T.V.W.Janssens, H.J.Jakobsen, J.Skibsted. *Microporous Mesoporous Mater.*, **39**, 393 (2000)
180. C.J.H.Jacobsen, C.Madsen, J.Houzvicka, I.Schmidt, A.Carlsson. *J. Am. Chem. Soc.*, **122**, 7116 (2000)
181. J.B.Koo, N.Jiang, S.Saravanamurugan, M.Bejblova, Z.Musilova, J.Cejka, S.E.Park. *J. Catal.*, **276**, 327 (2010)
182. K.Tang, Y.G.Wang, L.J.Song, L.H.Duan, X.T.Zhang, Z.L.Sun. *Mater. Lett.*, **60**, 2158 (2006)
183. L.Xu, S.Wu, J.Guan, H.Wang, Y.Ma, K.Song, H.Xu, H.Xing, C.Xu, Z.Wang, Q.Kan. *Catal. Commun.*, **9,** 1272 (2008)
184. Z.Hajjar, A.Khodadadi, Y.Mortazavi, S.Tayyebi, S.Soltanali. *Fuel*, **179**, 79 (2016)
185. R.Khare, A.Bhan. *J. Catal.*, **329**, 218 (2015)
186. Y.Wei, T.E.Parmentier, K.P.Jong, J.Zecevic. *Chem. Soc. Rev.*, **44**, 7234 (2015)
187. G.Hellmut, J.Weitkamp. *Molecular Sieves — Science and Technology*. Vol. 3. (Berlin, Heidelberg: Springer-Verlag, 2002). P. 452
188. H.Saitoa, S.Inagaki, K.Kojima, Q.Han, T.Yabe, S.Ogo, Y.Kubota, Y.Sekine. *Appl. Catal., A*, **549**, 76 (2018)
189. C.S.Triantafillidis, A.G.Vlessidis, N.P.Evmiridis. *Ind. Eng. Chem. Res.*, **39**, 307 (2000)

190. C.J.van Oers, W.J.J.Stevens, E.Bruijn, M.Mertens, O.I.Lebede, G.van Tendeloo, V.Meynen, P.Cool. *Microporous Mesoporous Mater*., **120**, 29 (2009)
191. Z.Xiaochun, W.Leilei, C.M.M.Pieter, M.Brahim, J.M.E.Hensen. *J. Catal*., **327**, 10 (2015)
192. E.Koohsaryan, M.Anbia. *Chin. J. Catal*., **37**, 447 (2016)
193. M.Ogura, S.Y.Shinomiya, J.Tateno, Y.Nara, E.Kikuchi, M.Matsukata. *Chem. Lett*., **29**, 882 (2000)
194. M.Ogura, S.Y.Shinomiya, J.Tateno, Y.Nara, M.Nomura, E.Kikuchi, M.Matsukata. *Appl. Catal., A*, **219**, 33 (2001)
195. T.Okuhara, T.Suzuki. *Microporous Mesoporous Mater*., **43**, 83 (2001)
196. J.C.Groen, J.C.Jansen, J.A.Moulijn, J.Perez-Ramírez. *J. Phys. Chem. B*, **108**, 13062 (2004)
197. K.H.Li, J.Valla, J.Garcia-Martinez. *ChemCatChem*, **6**, 46 (2014)
198. I.A.Ivanova, A.A.Kasyanov, V.I.Maerle, V.I.Zaikovskii. *Microporous Mesoporous Mater*., **189**, 163 (2014)
199. J.P.Na, G.Z.Liu, T.Y.Zhou, G.C.Ding, S.L.Hu, L.Wang. *Catal. Lett*., **143**, 267 (2013)
200. A.Charkhi, H.Kazemian, M.Kazemeini. *Powder Technol*., **203**, 389 (2010)
201. T.Wakihara, K.Sato, S.Inagaki, J.Tatami, K.Komeya, T.Meguro, Y.Kubota. *ACS Appl. Mater. Interfaces*, **2**, 2715 (2010)
202. S.V.Konnov, V.S.Pavlov, I.I.Ivanova, S.N.Khadzhiev. *Petrol. Chem*., **56**, 1154 (2016)
203. N.V.Kolesnichenko, S.V.Konnov, V.S.Pavlov, O.V.Yashina, N.N.Ezhova, S.N.Khadzhiev. *Petrol. Chem*., **57**, 576 (2017)
204. R.Liu, R.Liu, X.Ma, B.H.Davis, Zh.Li. *Fuel*, **211**, 827 (2018)
205. Q.Chen, G.Liu, Sh.Ding, M.Ch.Sheikh, D.Long, Y.Yoneyama, N.Tsubaki. *Chem. Eng. J*., **334**, 714 (2018)
206. Y.Chen, N.Batalha, M.Marinova, M.Impéror-Clerc, C.Ma, O.Ersen, W.Baaziz, J.A.Stewartf, D.Curulla-Ferré, A.Y.Khodakov, V.V.Ordomsky. *J. Catal*., **365**, 429 (2018)
207. A.P.Steynberg, S.R.Deshmukh, H.J.Robota. *Catal. Today*, **299**, 10 (2018)
208. H.Jahangiri, J.Bennett, P.Mahjoubi, K.Wilson, S.Gu. *Catal. Sci. Technol*., **4**, 2210 (2014)
209. Q.W.Sun. *Appl. Chem. Ind*., **35**, 212 (2006)
210. D.Xiang, S.Y.Yang, X.Liu, Y.Qian. *Chem. Eng. J*., **240**, 45 (2014)
211. M.Zhao, Y.Cui, J.Sun, Q.Zhang. *Catal. Today*, **316**, 142 (2018)
212. X.Gao, J.Zhang, N.Chen, Q.Ma, S.Fan, T.Zhao, N.Tsubaki. *Chin. J. Catal*., **37**, 510 (2016)
213. K.Asami, K.Komiyama, K.Yoshida, H.Miyahara. *Catal. Today*, **303**, 117 (2018)
214. Z.Tian, C.Wang, Z.Si, L.Ma, L.Chen, Q.Liu, Q.Zhang, H.Huang. *Appl. Catal. A: Gen*., **541**, 50 (2017)
215. Y.Cheng, J.Lin, T.Wu, H.Wang, S.Xie, Y.Pei, S.Yan, M.Qiao, B.Zong. *Appl. Catal., B*, **204**, 475 (2017)
216. H.M.Torres Galvis, A.C.J.Koeke, J.H.Bitter, T.Davidian, M.Ruitenbeek, A.I.Dugulan, K.P.de Jong. *J. Catal*., **303**, 22 (2013)
217. M.Oschatz, N.Krans, J.Xie, K.P.de Jong. *J. Energy Chem*., **25**, 985 (2016)
218. S.M.G.Lama, J.L.Weber, T.Heil, J.P.Hofmann, R.Yan, K.P.de Jong, M.Oschatz. *Appl. Catal., A*, **568**, 213 (2018)
219. H.Wang, J.Wang, Y.Yuan, Q.Zhao, X.Teng, S.Huang, X.Ma. *Catal. Today*, **314**, 101 (2018)
220. Z.Ni, H.Qin, S.Kang, J.Bai, Z.Wang, Y.Li, Z.Zheng, X.Li. *J. Colloid Interface Sci*., **516**, 16 (2018)
221. G.Liu, Q.Chen, E.Oyunkhand, S.Ding, N.Yamane, G.Yang, Y.Yoneyama, N.Tsubaki. *Carbon*, **130**, 304 (2018)
222. B.Gu, S.He, W.Zhou, J.Kang, K.Cheng, Q.Zhang, Y.Wang. *J. Energy Chem*., **26**, 608 (2017)
223. Y.Zhang, L.Ma, T.Wang, X.Li. *Catal. Commun*., **64**, 32 (2015)
224. J.Sun, Y.Chen, J.Chen. *Catal. Commun*., **91**, 34 (2017)
225. F.Jiao, J.Li, X.Pan, J.Xiao, H.Li, H.Ma, M.Wei, Y.Pan, Z.Zhou, M.Li, S.Miao, J.Li, Y.Zhu, D.Xiao, T.He, J.Yang, F.Qi, Q.Fu, X.Bao. *Science*, **351**, 1065 (2016)
226. Y.Zhu, X.Pan, F.Jiao, J.Li, J.Yang, M.Ding, Y.Han, Z.Liu, X.Bao. *ACS Catal*., **7**, 2800 (2017)
227. K.Cheng, B.Gu, X.Liu, J.Kang, Q.Zhang, Y.Wang. *Angew. Chem., Int. Ed*., **55**, 4725 (2016)
228. V.P.Santos, T.A.Wezendonk, J.J.D.Jaén, A.I.Dugulan, M.A.Nasalevich, H.U.Islam, A.Chojecki, S.Sartipi, X.Sun, A.A.Hakeem, A.C.J.Koeken, M.Ruitenbeek, T.Davidian, G.R.Meima, G.Sankar, F.Kapteijn, M.Makkee, J. Gascon. *Nat. Commun*., **6**, 6451(2015)
229. Z.Zhang, W.Dai, X.-Ch.Xu, J.Zhang, B.Shi, J.Xu, W.Tu, Y.F.Han. *AIChE J*., **63**, 4451 (2017)
230. D.Wang, B.Chen, X.Duan, D.Chen, X.Zhou. *J. Energy Chem*., **25**, 911 (2016)
231. K.Cheng, M.Virginie, V.V.Ordomsky, C.Cordier, P.A.Chemavskii, M.I.Ivantsov, S.Paul, Y.Wang, A.Y.Khodakov. *J. Catal*., **328**, 139 (2015)
232. R.Løden, O.Lunder, J.-E.Lein, P.I.Dahl, I.-H.Svenum. *Catal. Today*, **299**, 47 (2018)
233. M.Oschatz, J.P.Hofmann, T.W.V.Deelen, W.S.Lamme, N.A.Krans, E.J.M.Hensen, K.P.de Jong. *ChemCatChem*, **9**, 620 (2017)
234. L.M.Chew, W.Xia, H.Düdder, P.Weide, H.Ruland, M.Muhler. *Catal. Today*, **270**, 85 (2016)
235. J.Xie, J.Yang, A.I.Dugulan, A.Holmen, D.Chen, K.P.de Jong, M.J.Louwerse. *ACS Catal*., **6**, 3147 (2016)
236. J.Xie, H.M.Torres Galvis, A.C.J.Koeken, A.Kirilin, A.I.Dugulan, M.Ruitenbeek, K.P.de Jong. *ACS Catal*., **6**, 4017 (2016)
237. A.N.Pour, M.R.Housaindokht. *J. Nat. Gas Sci. Eng*., **14**, 204 (2013)
238. Z.Zhang, J.Zhang, X.Wang, R.Si, J.Xu, Y.F.Han. *J. Catal*., **365**, 71 (2018)
239. X.Duan, D.Wang, G.Qian, J.C.Walmsley, A.Holmen, D.Chen, X.Zhou. *J. Energy Chem*., **25**, 311 (2016)
240. H.M.Torres Galvis, J.H.Bitter, C.B.Khare, M.Ruitenbeek, A.I.Dugulan, K.P.de Jong. *Science*, **335**, 835 (2012)
241. C.M.Wang, Y.D.Wang, Z.K.Xie. *Catal. Sci. Technol*., **6**, 6644 (2016)
242. Y.Wang. *J. Energy Chem*., **25**, 169 (2016)
243. J.Su, D.Wang, Y.Wang, H.Zhou, C.Liu, S.Liu, C.Wang, W.Yang, Z.Xie, M.He. *ChemCatChem*, **10**, 1536 (2018)
244. F.Jiao, X.Pan, K.Gong, Y.Chen, G.Li, X.Bao. *Angew. Chem., Int. Ed*., **57**, 4692 (2018)
245. J.Wang, W.Zhou, J.Kang, K.Cheng, S.He, J.Shi, C.Zhou, Q.Zhang, J.Chen, L.Peng, M.Chen. *Angew. Chem., Int. Ed*., **57**, 12012 (2018)
246. G.Raveendra, C.Li, Y.Cheng, F.Meng, Z.Li. *New J. Chem*., **42**, 4419 (2018)
247. X.Liu, W.Zhou, Y.Yang, K.Cheng, J.Kang, L.Zhang, G.Zhang, X.Min, Q.Zhang, Y.Wang. *Chem. Sci*., **9**, 4708 (2018)
248. T.Qiu, L.Wang, S.Lv, B.Sun, Y.Zhang, Z.Liu, W.Yang, J.Li. *Fuel*, **203**, 811 (2017)
249. Y.J.Lee, J.Y.Park, K.W.Jun. *Catal. Lett*., **126**, 149 (2008)
250. J.Y.Park, Y.J.Lee, K.W.Jun, J.W.Bae, N.Viswanadham, Y.H.Kim. *J. Ind. Eng. Chem*., **15**, 847 (2009)
251. D.L.S.Nieskens, A.Ciftci, P.E.Groenendijk, M.F.Wielemaker, A.Malek. *Ind. Eng. Chem. Res*., **56**, 2722 (2017)
252. K.Cheng, W.Zhou, J.Kang, S.He, S.Shi, Q.Zhang, Y.Pan, W.Wen, Y.Wang. *Chem*, **3**, 334 (2017)
253. C.D.Chang, J.N.Miale, R.F.Socha. *J. Catal*., **90**, 84 (1984)
254. J.Bao, G.Yang, Y.Yoneyama, N.Tsubaki. *ACS Catal*., **9**, 3026 (2019)
255. X.P.Yang, L.Dong. *Chem. Ind. Eng. Prog*., **31**, 1726 (2012)
256. D.Xiang, S.Yang, Y.Qian. *Energy Conv. Manag*., **110**, 33 (2016)

257. R.Lin, A.P.Amrute, J.Pérez-Ramírez. *Chem. Rev.*, **117**, 4182 (2017)
258. V.Paunovic, G.Zichittella, M.Moser, A.P.Amrute, J.Perez-Ramirez. *Nat. Chem.*, **8**, 803 (2016)
259. Patent RU 2446881 (2012)
260. Z.Jiang, B.X.Shen, J.G.Zhao, L.Wang, L.T.Kong, W.G.Xiao. *Ind. Eng. Chem. Res.*, **54**, 12293 (2015)
261. J.Zheng, D.Jin, Z.Liu, K.Zhu, X.Zhou, W.Yuan. *Ind. Eng. Chem. Res.*, **57**, 548 (2018)
262. N.Li, Y.Y.Zhang, L.Chen, C.T.Au, S.F.Yin. *Microporous Mesoporous Mater.*, **227**, 76 (2016)
263. D.Wen, Q.Liu, Z.Fei, Y.Yang, Z.Zhang, X.Chen, J.Tang, M.Cui, X.Qiao. *Ind. Eng. Chem. Res.*, **57**, 446 (2018)
264. Q.Liu, D.Wen, Y.Yang, Z.Fei, Z.Zhang, X.Chen, J.Tang, M.Cui, X.Qiao. *Appl. Surf. Sci.*, **435**, 945 (2018)
265. M.Gamero, A.T.Aguayo, A.Ateka, P.Pérez-Uriarte, A.G.Gayubo, J.Bilbao. *Ind. Eng. Chem. Res.*, **54**, 7822 (2015)
266. M.Gamero, B.Valle, A.G.Gayubo, P.Castaåo, A.T.Aguayo, J.Bilbao. *Ind. Eng. Chem. Res.*, **57**, 908 (2018)
267. T.Xu, Q.Zhang, H.Song, Y.Wang. *J. Catal.*, **295**, 232 (2012)
268. T.Xu, H.Liu, Q.Zhao, S.Cen, L.Du, Q.Tang. *Catal. Commun.*, **119**, 96 (2019)
269. V.N.Rozanov, Yu.A.Treger, O.P.Murasheva, I.S.Silina, E.A.Averina. *Neftegasokhimiya*, **2**, 29 (2015)
270. Yu.A.Treger, V.N.Rozanov, S.V.Sokolova, O.P.Murasheva. *Kataliz v Khimicheskoi i Neftekhimicheskoi Promyshlennosti*, **3**, 15 (2012)
271. Patent RU 2451005 (2012)
272. Patent RU 2394805 (2010)
273. L.M.Kartashov, V.N.Rozanov, Yu.A.Treger, M.R.Flid, T.L.Kolyuzhnaya. *Kataliz v Promyshlennosti*, **3**, 36 (2010)
274. Patent RU 2522576 (2014)
275. J.He, T.Xu, Z.Wang, Q.Zhang, W.Deng, Y.Wang. *Angew. Chem., Int. Ed.*, **51**, 2438 (2012)
276. A.Vatani, E.Jabbari, M.Askarieh, M.A.Torangi. *J. Nat. Gas Sci. Eng.*, **20**, 347 (2014)
277. Patent US 8912381 (2014)
278. V.I.Alexiadis, T.Serres, G.B.Marin, C.Mirodatos, J.W.Thybaut, Y.Schuurman. *AIChE J.*, **64**, 2603 (2018)
279. A.G.Dedov, A.S.Loktev, N.O.Tel'Pukhovskaya, M.N.Kartasheva, M.V.Gerashchenko, I.I.Moiseev, K.V.Parkhomenko. *Petrol. Chem.*, **50**, 420 (2010)
280. B.M.Sollier, L.E.Gømez, A.V.Boix, E.E.Miry. *Appl. Catal., A*, **550**, 113 (2018)
281. F.Cheng, J.Yang, L.Yan, J.Zhao, H.Zhao, H.Song, L.Chou. *React. Kinet. Mech. Catal.*, **125**, 675 (2018)
282. L.Peng, J.Xu, X.Fang, W.Liu, X.Xu, L.Liu, Z.Li, H.Peng, R.Zheng, X.Wang. *Eur. J. Inorg. Chem.*, 1787 (2018)
283. C.Uzunoglu, A.Leba, R.Yildirim. *Appl. Catal., A*, **547**, 22 (2017)
284. V.I.Alexiadis, M.Chaar, A.van Veen, M.Muhler, J.W.Thybaut, G.B.Marin. *Appl. Catal., B*, **199**, 252 (2016)
285. Y.H.Hou, W.C.Han, W.S.Xia, H.L.Wan. *ACS Catal.*, **5**, 1663 (2015)
286. B.Beck, V.Fleisher, S.Arndt, M.G.Hevia, A.Urakawa, P.Hugo, R.Schomacher. *Catal. Today*, **228**, 212 (2014)
287. C.Karakaya, H.Zhu, B.Zohour, S.Senkan, R.J.Kee. *ChemCatChem*, **9**, 4538 (2017)
288. Y.Gordienko, T.Usmanov, V.Bychkov, V.Lomonosov, Z.Fattakhova, Y.Tulenin, D.Shashkin, M.Sinev. *Catal. Today*, **278**, 127 (2018)
289. A.Shubin, I.Zilberberg, I.Ismagilov, M.Kerzhentsev, Z.Ismagilov. *Mol. Catal.*, **445**, 307 (2018)
290. Z.Li, S.Wang, W.Hong, S.Zou, L.Xiao, J.Fan. *ChemNanoMat*, **4**, 487 (2018)
291. I.Z.Ismagilov, E.V.Matus, V.S.Popkova, V.V.Kuznetsov, V.A.Ushakov, S.A.Yashnik, I.P.Prosvirin, M.A.Kerzhentsev, Z.R.Ismagilov. *Kinet. Catal.*, **58**, 622 (2017)
292. X.Fang, S.Li, J.Lin, Y.Chu. *J. Mol. Catal. (China)*, **8**, 255 (1992)
293. V.Spallina, I.C.Velarde, J.A.M.Jimenez, H.R.Godini, F.Gallucci, M.van Sint Annaland. *Energy Convers. Manag.*, **154**, 244 (2017)
294. U.Zavyalova, M.Holena, R.Schlögl, M.Baerns. *ChemCatChem*, **3**, 1935 (2011)
295. H.R.Godini, A.Gili, O.Görke, S.Arndt, U.Simon, A.Thomas, R.Schomäcker, G.Wozny. *Catal. Today*, **236**, 12 (2014)
296. A.Aseem, G.G.Jeba, M.T.Conato, J.D.Rimer, M.P.Harold. *Chem. Eng. J.*, **331**, 132 (2018)
297. A.G.Dedov, A.S.Loktev, S.D.Golikov, N.A.Spesivtsev, I.I.Moiseev, G.D.Nipan, S.N.Dorokhov. *Petrol. Chem.*, **55**, 163 (2015)
298. V.Fleischer, P.Littlewood, S.Parishan, R.Schomäcker. *Chem. Eng. J.*, **306**, 646 (2016)
299. L.Zeng, Z.Cheng, J.A.Fan, L.S.Fan, J.Gong. *Nature Rev. Chem.*, **2**, 349 (2018)
300. S.Parishan, P.Littlewood, A.Arinchtein, V.Fleischer, R.Schomäcker. *Catal. Today*, **311**, 40 (2018)
301. V.Fleischer, U.Simon, S.Parishan, M.G.Colmenares, O.Görke, A.Gurlo, W.Riedel, L.Thum, J.Schmidt, Th.Risse, K.P.Dinse, R.Schomäcker. *J. Catal.*, **360**, 102 (2018)
302. E.Y.Chung, W.K.Wang, S.G.Nadgouda, D.S.Baser, J.A.Sofranko, L.-Sh.Fan. *Ind. Eng. Chem. Res.*, **55**, 2750 (2016)
303. Zh.Cheng, D.S.Baser, S.G.Nadgouda, L.Qin, J.A.Fan, L.-Sh.Fan. *ACS Energy Lett.*, **3**, 1730 (2018)
304. A.Aseem, M.P.Harold. *Chem. Eng. Sci.*, **175**, 199 (2018)
305. J.Garcia-Fayos, M.P.Lobera, M.Balaguer, J.M.Serra. *Front. Mater.*, **5**, 1 (2018)
306. S.Bhatia, C.Y.Thien, A.R.Mohamed. *Chem. Eng. J.*, **148**, 525 (2009)
307. N.H.Othman, Z.Wu, K.Li. *J. Membr. Sci.*, **488**, 182 (2015)
308. V.O.Igenegbai, R.J.Meyer, S.Linic. *Appl. Catal., B*, **230**, 29 (2018)
309. D.E.Sommer, P.Kirchen. *Chem. Eng. Sci.*, **195**, 11 (2019)
310. Patent US 8962517 (2015)
311. J.Song, Y.Sun, R.Ba, Sh.Huang, Y.Zhao, J.Zhang, Y.Sun, Y.Zhu. *Nanoscale*, **7**, 2260 (2015)
312. Patent RU 2515497 (2014)
313. S.Delavari, N.A.S.Amin, H.Mazaheri. *React. Kinet. Mech. Catal.*, **113**, 557 (2014)
314. G.D.Nipan. *Inorg. Mater.*, **51**, 389 (2015)
315. G.D.Nipan. *Inorg. Mater.*, **54**, 96 (2018)
316. V.I.Lomonosov, M.Y.Sinev. *Kinet. Catal.*, **57**, 647 (2016)
317. V.I.Lomonosov, Y.A.Gordienko, M.Y.Sinev, V.A.Rogov, V.A.Sadykov. *Russ. J. Phys. Chem. A*, **92**, 430 (2018)
318. C.Karakaya, H.Zhu, C.Loebick, J.G.Weissman, R.J.Kee. *Catal. Today*, **312**, 10 (2018)
319. R.J.Kee, C.Karakaya, H.Zhu. *Proc. Combust. Inst.*, **36**, 51 (2017)
320. *Siluria Technologies. Demonstration Plant*. http://siluria.com/Technology/Demonstration_Plant (Last accessed 27.01.2020)
321. Patent US 9334204 (2016)
322. Patent US 9352295 (2016)
323. Patent US 9567269 (2017)
324. Patent US 10047020 (2018)
325. R.T.Yunarti, M.Lee, Y.J.Hwang, J.W.Choi, D.J.Suh, J.Lee, I.W.Kim, J.-M.Ha. *Catal. Commun.*, **50**, 54 (2014)
326. T.W.Elkins, S.J.Roberts, H.E.Hagelin-Weaver. *Appl. Catal., A*, **528**, 175 (2016)
327. F.Bo, J.Tao, Z.Yan. *J. Nanosci. Nanotechnol.*, **18**, 3398 (2018)
328. T.Jiang, J.Song, M.Huo, N.T.Yang, J.Liu, J.Zhang, Y.Sun, Y.Zhu. *RSC Adv.*, **41**, 34872 (2016)
329. P.Huang, Y.Zhao, J.Zhang, Y.Zhu, Y.Sun. *Nanoscale*, **5**, 10844 (2013)
330. Z.Liu, J.P.H.Li, E.Vovk, Y.Zhu, S.Li, S.Wang, A.P.v.Bavel, Y.Yang. *ACS Catal.*, **8**, 11761 (2018)
331. D.Noon, A.Subsai, S.Senkan. *ChemCatChem,* **5**, 146 (2013)
332. Patent RU 2647844 (2018)

333. W.Jeon, J.Y.Lee, M.Lee, J.-W.Choi, J.-M.Ha, D.J.Suh, I.W.Kim. *Appl. Catal., A*, **464** – **465**, 68 (2013)
334. P.Wang, X.Zhang, G.Zhao, Y.Liu, Y.Lu. *Chin. J. Catal.*, **39**, 1395 (2018)
335. W.Liang, S.Sarsani, D.West, A.Mamedov, I.Lengyel, H.Perez, J.Lowrey. *Catal. Today*, **299**, 60 (2018)
336. N.P.Kirik, N.N.Anshits, E.V.Rabchevskii, L.A.Solovyov. *J. Siber. Feder. Univ. Chem.*, **11**, 347 (2018)
337. M.Haneda, Y.Katsuragawa, Y.Nakamura, A.Towata. *Front. Chem.*, **6**, 581 (2018)
338. C.Chu, Y.Zhao, S.Li, Y.Sun. *Phys. Chem. Chem. Phys.*, **18**, 16509 (2016)
339. J.Xu, A.Zheng, X.Wang, G.Qi, J.Su, J.Du, Z.Gan, J.Wu, W.Wang, F.Deng. *Chem. Sci.*, **3**, 2932 (2012)
340. N.Kosinov, F.J.A.G.Coumans, E.A.Uslamin, A.S.G.Wijpkema, B.Mezari, E.J.M.Hensen. *ACS Catal.*, **7**, 520 (2017)
341. D.B.Lukyanov, T.Vazhnova. *J. Mol. Catal. A: Chem.*, **342** – **343**, 1 (2011)
342. M.V.Tsodikov, Y.V.Slivinskii, V.P.Mordovin, O.V.Bukhtenko, G.Colon, M.C.Hidalgo, J.A.Navio. *Chem. Commun.*, **4**, 943 (1999)
343. M.V.Tsodikov, V.Ya.Kugel, F.A.Yandieva, E.V.Slivinskii, I.I.Moiseev, G.Colon, M.C.Hidalgo, J.A.Navio. *Stud. Surf. Sci. Catal.*, **138**, 239 (2001)
344. X.Guo, G.Fang, G.Li, H.H.Ma, H.Fan, L.Yu, C.Ma, X.Wu, D.Deng, M.Wei, D.Tan, R.Si, S.Zhang, J.Li, L.Sun, Z.Tang, X.Pan, X.Bao. *Science*, **344** , 616 (2014)
345. M.Sakbodin, Y.Wu, S.C.Oh, E.D.Wachsman, D.Liu. *Angew. Chem., Int. Ed.*, **55**, 16149 (2016)
346. T.Minea, D.C.M.van den Bekerom, F.J.J.Peeters, E.Zoethout, M.F.Graswinckel, M.C.M.van de Sanden, T.Cents, L.Lefferts, G.J.van Rooij. *Plasma Proc. Polym.*, **15**, 1800087 (2018)